Quantitative Endoproteinase GluC Footprinting of Cooperative Ca^{2+} Binding to Calmodulin: Proteolytic Susceptibility of E31 and E87 Indicates Interdomain Interactions†

Susan Pedigo and Madeline A. Shea*

Department of Biochemistry, University of Iowa College of Medicine, Iowa City, Iowa 52242-1109

Received July 19, 1994; Revised Manuscript Received October 25, 1994®

ABSTRACT: Calmodulin is the primary eukaryotic intracellular calcium receptor. Cooperative calcium binding to two sites in each of two domains drives large conformational changes that enable it to activate target proteins. An understanding of the molecular mechanism of cooperativity requires determination of the conformational states populated by calmodulin, the intrinsic free energies of binding calcium to four sites, and the nature and degree of intradomain and interdomain interactions. To monitor residue-specific conformational changes within calmodulin as calcium binds, we have developed a new quantitative proteolytic footprinting method using endoproteinase GluC (EndoGluC). Under conditions of very limited proteolysis, cleavage occurred at only five of the sixteen positions possible in calmodulin. The relative abundance of fragments indicated that calcium induced changes in the susceptibility of individual peptide bonds. Quantitative susceptibility profiles were resolved for two positions: E31-L32, in site I in the N-terminal domain, and E87-A88, preceding site III in the C-terminal domain. In apocalmodulin, E87-A88 was susceptible to EndoGluC; calcium binding to sites III and IV caused monotonic protection from proteolysis. The response of E31-L32 was biphasic. In apocalmodulin, it was resistant to cleavage. Susceptibility was induced by calcium binding to sites III and IV, followed by protection induced by calcium binding to sites I and II. This indicated that calmodulin must adopt at least three distinguishable conformations and suggested that the two domains interact. Model-dependent equilibrium constants were resolved from the EndoGluC susceptibility profiles for E31 and E87; they indicated cooperative binding within each domain. Approaches taken to validate this proteolytic footprinting method are described.

Calmodulin (CaM),[1] an essential element in most calcium-mediated signal transduction pathways, binds calcium cooperatively in response to an increase in intracellular calcium concentration. The binding of calcium is understood to cause conformational changes that expose hydrophobic surfaces (LaPorte *et al.*, 1980) and allow calmodulin to activate tissue-specific target proteins that regulate a myriad of cellular processes [see Cohen and Klee (1988) and Török and Whitaker (1994)]. Despite many years of careful experimental studies and theoretical modeling [see Weinstein and Mehler (1994) for a recent review], there is much to be learned about the cooperative mechanism of calcium binding to calmodulin and the extent to which sites and domains may interact. This study describes the development of an approach to quantitatively monitor residue-specific conformational switching induced by calcium binding to calmodulin (in the absence of target proteins). The goal is to determine the number and properties of the molecular states populated by calmodulin and to determine the rules of calcium-driven transition between them.

Although calmodulin in the size of only a single subunit of hemoglobin, it contains four ligand binding sites in a highly conserved (Moncrief *et al.*, 1990) and repetitive amino acid sequence configured in an $\alpha-\beta-\alpha'-\beta'$ pattern, as shown in Figure 1a. This arrangement has confounded attempts to use optical spectroscopy to monitor individual binding sites of the native protein because each segment does not have a unique reporter group. High-resolution structural studies [Babu *et al.*, 1988; Ikura *et al.*, 1991; see McPhalen *et al.* (1991) for a review] have shown that each of the four segments of calcium-saturated calmodulin does contain a very similar helix−loop−helix or EF-hand calcium binding site motif [see Kretsinger (1976)]. A short region of β-sheet exists between sites I and II in the amino-terminal (N-terminal) domain (residues 1−75) and between sites III and IV in the carboxyl-terminal (C-terminal) domain (residues 76−148). No structural models of comparable resolution have been determined for apocalmodulin, although spectroscopic studies suggest that it is generally more disordered while retaining two pairs of EF-hand sites (Hoffman & Klevit, 1991; Finn *et al.*, 1993; Drabikowski & Brzeska, 1982).

† These studies were supported by grants to M.A.S. from the American Heart Association (910148980), the National Science Foundation Presidential Young Investigator Award (NSF MCB 9057157), and the NIH Diabetes and Endocrinology Research Center (DK 25295). S.P. was supported by an NIH Predoctoral Traineeship in Biotechnology (PHS 1 T32 GM08365-04).

* Corresponding author. Telephone: (319) 335-7885. e-mail: madeline-shea@uiowa.edu.

® Abstract published in *Advance ACS Abstracts,* January 1, 1995.

[1] Abbreviations: CaM, calmodulin; Z-FLE-NA, (carbobenzoxy)-phenylalanyl-L-leucyl-L-α-glutamyl-4-nitroanilide; CD, circular dichroism; EndoGluC, endoproteinase GluC; EGTA, ethylene glycol bis(β-aminoethyl ether)-*N,N,N′,N′*-tetraacetic acid; HEPES, *N*-(2-hydroxyethyl)piperazine-*N′*-2-ethanesulfonic acid; HPLC, high-performance liquid chromatography; IPTG, isopropyl β-D-thiogalactopyranoside; KCl, potassium chloride; NTA, nitrilotriacetic acid; NMR, nuclear magnetic resonance; TFAA, trifluoroacetic acid; BAPTA, 1,2-bis(*O*-aminophenoxy)ethane-*N,N,N′,N′*-tetraacetic acid.

0006-2960/95/0434-1179$09.00/0

FIGURE 1: (a) Amino acid sequence of rat and bovine calmodulin. The sequence was divided into segments. Segment α (residues 1−39) includes site I; segment β (residues 40−75) includes site II; segment α' (residues 76−112) includes site III; segment β' (residues 113−148) includes site IV. The 12 residues of the calcium binding sites (boxed residues) are aligned. The subset of glutamate residues (E) that are possible cleavage sites for EndoGluC is indicated in shaded boxes. (b) Depiction of $(Ca^{2+})_4$-CaM crystal structure (Babu *et al.*, 1988) showing E31 and E87, two positions of cleavage by EndoGluC. Coordinates are taken from Brookhaven Protein Data Bank file 3cln.pdb (Bernstein *et al.*, 1977; Abola *et al.*, 1987); ribbon drawing of the backbone was made using MolScript (Kraulis, 1991). The secondary structure type of the central helix is based on studies by Ikura *et al.* (1991).

Cooperative ligand binding to regulatory proteins is notoriously challenging to understand quantitatively because the partially liganded species of the protein are present in low abundance over the course of a titration. Many models of intradomain and interdomain cooperativity have been proposed [see Kilhoffer *et al.* (1992) for a review]. There is widespread agreement that (a) there are two classes of sites with macroscopic binding affinities that differ by approximately an order of magnitude and that (b) calcium binds to sites III and IV with higher affinity and apparently greater cooperativity than it does to sites I and II (Wang, 1985; Crough & Klee, 1980; Drabikowski & Brzeska, 1982; Starovasnik *et al.*, 1992; Martin *et al.*, 1985; Klee, 1977). From studies of calmodulin mutants, there is additional evidence that suggests that the intrinsic affinities of calcium binding sites within the same domain are not identical (Starovasnik *et al.*, 1992; Kilhoffer *et al.*, 1992).

Many studies concluded that there was little or no interaction between the N-terminal and C-terminal domains in the absence of target peptides or drugs [see Weinstein and Mehler (1994)]. However, chemical cross-linking (Persechini & Kretsinger, 1988; Small & Anderson, 1988), low-angle X-ray scattering (Heidorn & Trewhella, 1988), and other spectroscopic studies (Török *et al.*, 1992), as well as molecular modeling studies (Pascual-Ahuir *et al.*, 1991), have suggested that the central helix is actually flexible (Kretsinger, 1992b). Thus, it must be possible for the two domains of calmodulin to approach each other more closely than the distance observed in the crystallographic structure of $(Ca^{2+})_4$-CaM (Babu *et al.*, 1988) shown in Figure 1b. NMR studies showed that a portion of the central helix is nonhelical (Ikura *et al.*, 1991; Barbato *et al.*, 1992) in solution. Chemical modification and partial proteolysis have shown that there are calcium-dependent differences in the reactivity or accessibility of amino acid side chains in calmodulin that correlated with zero, two, and four calcium ions bound (Giedroc *et al.*, 1985, 1987; Mackall & Klee, 1991; Kawasaki *et al.*, 1986; Walsh *et al.*, 1977). These support a model having at least one intermediate state of the protein.

Although a cooperative molecular binding transition is best studied directly, that is rarely straightforward. In the case of hemoglobin, an understanding of the molecular mechanism of cooperativity and the inadequacy of 2-state models has required decades. Recent advances have required the development of new methods capable of probing the eight intermediate (partially liganded) species *via* the use of stable ligand analogs, mutant hemoglobins, and innovative trapping methods such as cryogenic isoelectric focusing [see Ackers and Hazzard (1993) for a review]. In the case of calmodulin, there are 14 partially liganded states (those having one, two, or three calcium ions bound). To identify which of these are populated significantly as calcium binds to calmodulin, we have embarked on a program to use many specific and nonspecific proteases to probe ligand-linked conformational change quantitatively.

There are many precedents for studying conformational switching in cooperative systems by probing ligand-induced changes in macromolecular susceptibility to enzymatic cleavage or chemical reactivity [e.g., the quantitative DNase footprint titration method, as developed by the laboratory of Ackers (Brenowitz *et al.*, 1986)]. The strength of an approach using limited proteolysis to probe calcium-linked conformational changes is that many positions of the native protein may be studied simultaneously without modification or mutation and without bias for the location of responses. This screening is essential in a protein the size of calmodulin, because most mutations studied to date affect more than one attribute (e.g., stability as well as calcium binding). In the absence of knowledge about residue-specific roles in conformational switching, it is extremely challenging to apply experimental methods of protein engineering fruitfully to test hypotheses based on high-resolution structures. It is not yet possible to accurately predict the free energies of binding and cooperative interactions on the basis of such structures.

The goal of this research was to monitor properties that would represent individual site binding isotherms reflecting the population distribution of partially saturated species. The challenge was to find properties of the native protein that

would indicate residue-specific conformational change in response to calcium binding. The consensus sequence (D-X-D-G-D/N-G-X_5-E) of the calcium binding sites has an invariant glutamate as the C-terminal residue (Figure 1a). This terminal glutamate residue offers both of its side chain oxygens for bidentate chelation of the calcium ion (Babu *et al.*, 1988). In addition to these four critical glutamate residues in the binding sites, seventeen others are distributed throughout the calmodulin sequence. Thus, EndoGluC was chosen as an enzymatic probe of calcium-induced changes in the conformation of calmodulin.

In this report, we describe the first use of EndoGluC to quantitatively determine (a) the positions of calcium-sensitive peptide bonds within calmodulin under conditions of limited proteolysis and (b) the fractional change in the calcium-dependent susceptibility of those bonds over the course of an equilibrium titration. The resolved susceptibility profiles were analyzed according to two simple binding models. The estimates of binding free energies are compared to those obtained from several independent methods used to monitor calcium binding. Validation of the EndoGluC footprinting method is described.

EXPERIMENTAL PROCEDURES

Materials

Recombinant rat calmodulin was overexpressed in *Escherichia coli* using the T7-7 vector (Tabor & Richardson, 1985) in Lys-S cells (U.S. Biochemicals, Cleveland, OH); this construct was the kind gift of R. Mauer and P. Howard. Recombinant calmodulin differs from tissue-derived calmodulin in that the N-terminus is unacetylated and K115 is not trimethylated. The recombinant protein was purified *via* phenyl Sepharose CL-4B (Pharmacia, Piscataway, NJ) chromatography (Putkey *et al.*, 1985) to approximately 99% purity, as judged by silver staining of overloaded denaturing gel electrophoresis experiments and small zone chromatography on a Superdex75 column (Pharmacia). The protein was chemically characterized by N-terminal sequencing and amino acid analysis (see the following section). Spectral characterization of the recombinant calmodulin included UV/vis, circular dichroism, and intrinsic tyrosine fluorescence spectroscopy as a function of calcium concentration. The ability of the recombinant rat calmodulin to stimulate phosphodiesterase activity was confirmed. Fluorimetric calcium probes, BAPTA and 4,4′-difluoro-BAPTA, were purchased from Molecular Probes (Eugene, OR). Endoproteinase GluC (EC 3.4.21.19, EndoGluC) was purchased from Promega (Madison, WI). (Carbobenzoxy)phenylalanyl-L-leucyl-L-α-glutamyl-4-nitroanilide (Z-FLE-NA), the substrate for EndoGluC activity, was purchased from Boehringer Mannheim Biochemicals (Indianapolis, IN). Solvents for HPLC and other routine laboratory chemicals were of the highest grade commercially available.

Methods

Calmodulin was equilibrated *via* extensive dialysis in a series of buffers of experimentally determined free calcium concentration. Each dialysate was then subjected to limited proteolysis. The proteolytic products were separated and quantified. The fractional abundance of each peptide was calculated and plotted against the concentration of free calcium in the buffer. These susceptibility profiles are a quantitative measure of the calcium-dependent accessibility of a specific peptide bond. The details of the experimental protocol and data analysis are described in the following sections.

Calcium/pH Buffers. All proteolyses were done in pH/pCa buffers containing 50 mM HEPES, 94 mM KCl, 0.5 mM EGTA, and 0.5 mM NTA. By the addition of calcium chloride ($CaCl_2$), 19 separate calcium buffers were prepared; they spanned a range from approximately nanomolar (pCa = 9) to millimolar (pCa = 3) free calcium concentration (pCa denotes $-\log [Ca^{2+}]_{free}$). All buffers were pH 7.40 ± 0.01 at 22.0 °C. The total calcium concentration was determined by atomic absorption spectroscopy. The concentration of KCl was determined with a CDM83 conductivity meter by Radiometer (Copenhagen).

The free calcium concentration in each of the buffers was determined experimentally by measuring the calcium-sensitive fluorimetric signal of 7 μM BAPTA (for buffers in the pCa range 9−6.4) or difluoro-BAPTA (buffers in the pCa range 6.7−5.5) to determine its degree of saturation and using that value to calculate the pCa (Swenson & Fredricksen, 1992). The dissociation constants (K_d) for calcium binding to each of these fluorophores were determined in our buffer system (see Figure 2a). Each pCa buffer was monitored by an SLM 4800 fluorimeter set at excitation and emission wavelengths of 255 and 364 nm for BAPTA and 257 and 369 nm for difluoro-BAPTA, respectively. These wavelengths were chosen to avoid spectral overlap when used in dialysates containing both a fluorophore and calmodulin (see the following). Fluorescence of the calcium-sensitive fluorophores decreased upon calcium binding. For each pCa buffer, the fluorescence of the added fluorophore (F_i) was compared to values of the end point fluorescence. The fluorescence signal of calcium-free fluorophore (F_{max}) was determined by adding EGTA to a total concentration of 3 mM; the fluorescent signal of calcium-saturated fluorophore (F_{min}) was determined by adding concentrated calcium chloride to a final concentration of 20 mM. The free calcium concentration of the buffer was calculated using the experimental values (F_i, F_{max}, and F_{min}) in eq 1.

$$[Ca^{2+}]_{free} = K_d(F_{max} - F_i)/(F_i - F_{min}) \qquad (1)$$

For buffers with high free calcium concentrations (buffers in the pCa range 5.2−3.5), the free calcium was determined using a calcium-selective electrode (F2110Ca) from Radiometer. The selectrode was calibrated with standards prepared from the Calcium Reference Solution (1000 ppm ± 1%) from Fisher. The experimentally determined values were compared to values calculated on the basis of published association constants (Fabiato & Fabiato, 1979; Sillen & Martell, 1971) using our own program based on standard equations of ionic equilibria. The buffers contained no added magnesium. Although magnesium is recognized to affect calcium binding to calmodulin and to be of physiological significance, it was omitted from these buffers to simplify the development of the EndoGluC footprinting method. Magnesium contamination in the buffers was estimated *via* atomic absorption analysis to be between 5 and 13 μM. These concentrations are well below the magnesium affinity of the calcium binding sites in calmodulin (Haiech *et al.*, 1981).

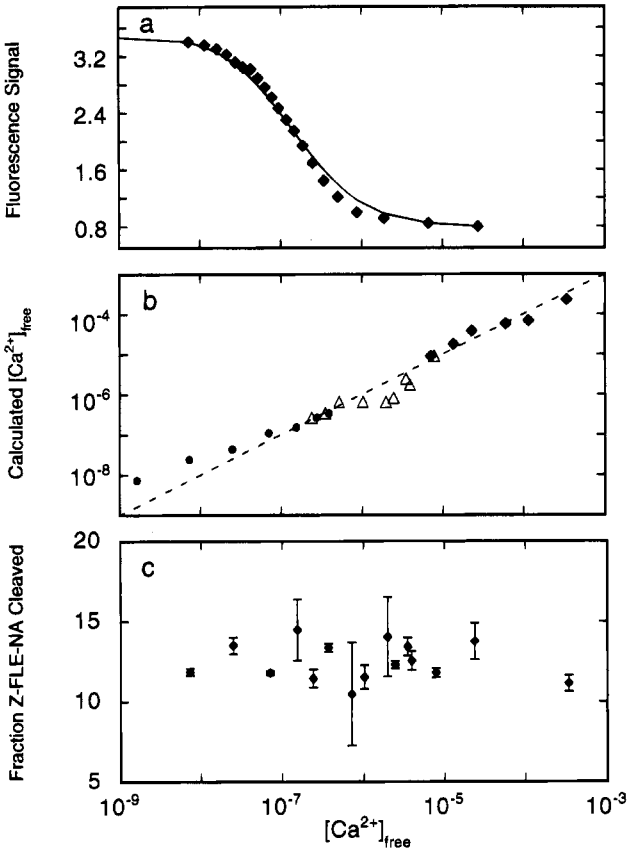

FIGURE 2: (a) Representative Ca^{2+} titration of BAPTA for the determination of dissociation constant. A solution of 4 μM BAPTA in 50 mM HEPES, 94 mM KCl, 0.5 mM NTA, and 0.5 mM EGTA, pH 7.40 at 22 °C, was titrated with calcium chloride and monitored fluorimetrically. The curve was simulated using the value of K_d resolved from a nonlinear least-squares analysis of the data according to a single site model (standard Langmuir binding isotherm). The results from triplicate determinations were K_d(BAPTA) = (1.26 ± 0.14) × 10^{-7} M and K_d(difluoro-BAPTA) = (7.9 ± 1.5) × 10^{-7} M. (b) Comparison of experimentally determined free calcium to the calculated free calcium concentration (dashed line) for each of the pCa/pH buffers. The ordinate free calcium values were calculated using published association constants (Fabiato & Fabiato, 1979; Sillen & Martell, 1971), and total calcium concentrations were measured by atomic absorption (see Experimental Procedures). The experimental free calcium values were determined by two approaches: fluorimetrically *via* the extrinsic calcium probes BAPTA (●) or difluoroBAPTA (○) or with a calcium-selective electrode (◆). (c) EndoGluC activity is independent of calcium concentration. The percent cleavage of the chromogenic substrate (Z-FLE-NA), determined by HPLC, is plotted *vs* the free calcium concentration for each of the 15 dialysates used in the proteolytic probe experiment. Each point represents the average and standard deviation of triplicate determinations.

Equilibration of Calmodulin. To conduct a discontinuous titration, calmodulin was dialysed extensively against each of the 19 separate pCa/pH buffers (1:30 ratio of dialysate to buffer in each of six buffer exchanges). The final concentration of calmodulin in each of these dialysates was estimated using an extinction coefficient of 3300 M^{-1} cm^{-1} at 277 nm (Klee, 1977), which agreed well with the concentration determined by amino acid analysis. Individual dialysates varied between 0.3 and 0.8 mg/mL (18−48 μM); they were aliquoted and stored at −20 °C. As judged by SDS−PAGE analysis, no degradation of the calmodulin was observed under these storage conditions.

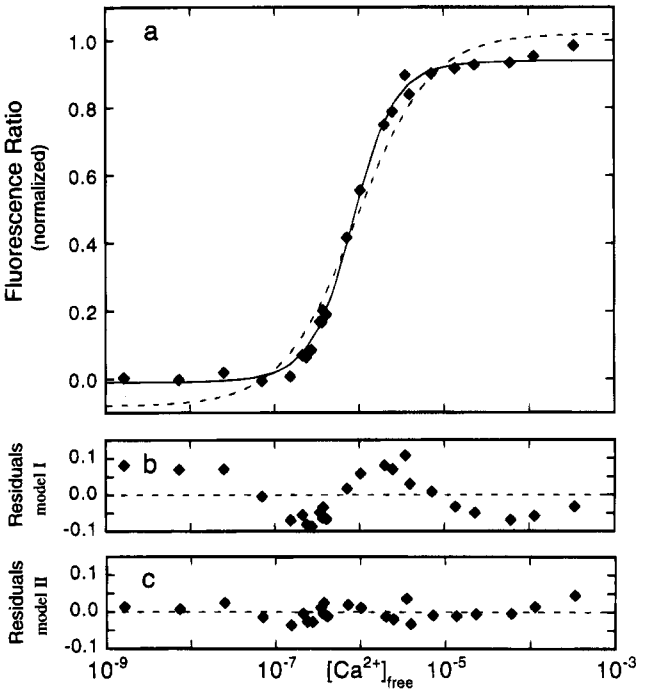

FIGURE 3: (a) Normalized calmodulin tyrosine fluorescence of each of 19 calmodulin dialysates. Excitation wavelength was 277 nm; emission was monitored at 308 nm. [CaM] was approximately 30 μg/mL (18 μM) in all samples. Buffer was 50 mM HEPES, 94 mM KCl, 0.5 mM EGTA, and 0.5 mM NTA, pH 7.40 at 22 °C, with varying amounts of free calcium (see Experimental Procedures). The value of free calcium for each dialysate (the abscissa) was calculated from simultaneously determined fluorescent signals of a fluorimetric probe (BAPTA or difluoro-BAPTA). Curves correspond to simulations using model I (eq 4, dashed line) or model II (eq 5, solid line) according to the best-fit values in Table 1. The Hill coefficient for these data was 1.7. (b) Residuals between the data and best fit to model I. (c) Residuals between the data and best fit to model II.

Calmodulin Fluorescence. The intrinsic tyrosine fluorescence of calmodulin was monitored in each of the 19 individual calmodulin dialysates; wavelengths were 277 nm for excitation and 308 nm for emission. The procedure was identical to that outlined for the determination of free calcium in the buffers used for dialysis. BAPTA or difluoro-BAPTA was added to 4 μM final concentration; multiple measurements of the same sample with different wavelengths gave the fluorescence of calmodulin and the fluorophore. The high- and low-fluorescence end points for each dialysate were determined by the addition of EGTA or excess calcium, as described earlier. In order to correct for variations in the concentration of calmodulin in different dialysates, the tyrosine fluorescence of an individual dialysate was normalized to its end points of high and low fluorescence. The resolved values of the normalized fluorescence, F_N, are shown in Figure 3. The calculated degree of saturation of BAPTA or difluoro-BAPTA was used to determine the free calcium concentration in each dialysate for comparison to the original buffer.

Proteolysis. All proteolyses and chromatographic separations were automated by the Gilson HPLC autosampler (see the following). Limited proteolysis was performed by precise volumetric addition of the EndoGluC stock solution (0.1 mg/mL) to the calmodulin dialysates. The total time of exposure was 18 min at 22 °C, as controlled by a water-jacketed autosampler rack. An internal standard for protease

activity, Z-FLE-NA, was added to a final concentration of 32 μM after 15 min for the last 3 min of proteolysis. Method development for the chromatography of the internal standard was done in the absence of calmodulin to ensure unambiguous identification of intact Z-FLE-NA and its two proteolytic products. The proteolytic footprinting reaction was quenched by injection of the mixture onto the HPLC column (see details in the following). The ratio of EndoGluC to calmodulin was 1:100 mass ratio (1:156 mol ratio). Prior to exposure to EndoGluC, dialysates were adjusted so that the concentration of calmodulin in each reaction was 14.4 μM. A volume of 100 μL (25 μg) was injected onto the column. Triplicate independent footprinting reactions were conducted using each dialysate. A total of 15 dialysates was used in the proteolytic probe experiments.

The proteolysis conditions were chosen such that the extent of cleavage of whole calmodulin was low (<15%) and the likelihood of multiple cleavage events of the fragments was reduced. EndoGluC is a serine protease that contains no divalent metal ions for structural or catalytic purposes. The dependence of proteolytic activity on calcium concentration was tested experimentally using the chromophoric substrate Z-FLE-NA.

Chromatography. EndoGluC footprinting reactions were analyzed chromatographically on an HPLC from Gilson Medical Electronics (Middleton, WI) consisting of Models 302 and 305 pumps, a Model 811 dynamic mixer equipped with a 700 μL mixing chamber, a Model 116 dual wavelength detector set at 220 and 344 nm, and a Model 231 autosampler. As mentioned previously, the versatility of the autosampler allowed the automation of all procedures required for proteolytic and chromatographic experiments. The column used for peptide separations was a Vydac C-18, 22 cm × 4.6 mm i.d. (Hesperis, CA). A binary solvent system of water (A) and 80:20 acetonitrile/water (B) with 0.06% TFAA added to each was used with the following gradients: 10% to 28% B from 3 to 8 min, 28% to 51% B from 8 to 28 min, 51% to 56% B from 28 to 42 min. The flow rate was 1 mL/min. Due to slight variations in the chromatography, peptide peaks were followed on the basis of the elution profile rather than strictly by their retention time.

To identify the proteolytic products, peptide peaks from the chromatograph were collected from the column effluent. The samples were dried and subsequently hydrolyzed in 6 N HCl under argon. Analysis of the amino acids in the hydrolysate was done on a Beckman 6300 amino acid analyzer at the Protein Structure Facility at the University of Iowa (data not shown). In no case was the identity of reported proteolytic fragments ambiguous.

Resolution of Proteolytic Susceptibility Profiles. The precision of integration of peak areas in a chromatogram depends on the precision of estimates of background absorbance as well as peak separation. The chromatographic method was optimized to resolved primary cleavage products. Peak area at 220 nm was determined for all peptides in the analysis. All automatic calculations of peak area were checked by an operator; modified corrections for baseline variations were applied when necessary. The fractional area percent of each peptide (A_i) was determined by

$$A_i = \frac{\text{peak area of peptide } i}{\text{peak area of CaM and all its peptide fragments}} \quad (2)$$

where the denominator is the sum of the peak areas for all calmodulin peptides and whole calmodulin (i.e., it represents the total mass of CaM in the footprinting reaction).

The activity of EndoGluC in each footprinting reaction was determined by a chromatographic assay of the proteolytic products formed by cleavage by Z-FLE-NA. The chromogenic portions of cleaved and uncleaved Z-FLE-NA have equal molar absorptivities at 344 nm, but distinct retention times in the HPLC chromatographic experiments (12 and 45 min, respectively). The exposure to protease was determined by the calculation of the ratio of the cleaved substrate relative to the total amount of chromogenic substrate as measured by peak area at 344 nm. The fraction of peptide i, A_i, was corrected for the fraction of Z-FLE-NA cleaved in that footprinting reaction according to

$$A_i' = A_i/(\text{fraction of Z-FLE-NA cleaved}) \quad (3)$$

Susceptibility profiles were generated by plotting the corrected fraction for each peptide, A_i', against the free calcium concentration of the dialysate.

Data Analysis. Footprinting titrations for each peptide consisted of triplicate independent determinations of EndoGluC susceptibility (A_i') for each of 15 calmodulin dialysates. All 45 data points were included in each fit. The independent variable, concentration of free calcium, was assumed to be known precisely. Susceptibility profiles and fluorescence signals were fit using *nonlin* (Johnson & Frasier, 1985), a nonlinear least-squares algorithm that uses a modified Gauss−Newton procedure for obtaining convergence to the best-fit parameters and provides multiple criteria for the evaluation of goodness-of-fit. The fitting was done using a Silicon Graphics Personal Iris workstation; Fortran functions were written to correspond to the following equations.

As required in all approaches to parameter estimation, it is necessary to make an assumption about the relationship between the experimental signal (A_i' or F_N) and the chemical model being tested. For the purposes of model-dependent analysis, we have postulated that the susceptibility of a peptide bond or intrinsic fluorescence is linearly related to the degree of binding. This is a standard approximation when using spectroscopic probes of binding. Problems with this convention will be discussed.

Despite the goal of understanding the cooperative mechanism of calcium binding to four interacting sites, the footprinting titrations provided constraints sufficient only to discriminate between two simple binding models. Model I treated the two sites of a domain as equal and independent (eq 4); this model may apply to a macromolecule with any number of binding sites, but was interpreted here in terms of the pair of sites within a globular domain.

$$\bar{Y}_I = \frac{K_1[X]}{1 + K_1[X]} \quad (4)$$

In this equation, K_1 is the intrinsic association constant for a site ($\Delta G_1 = -RT \ln K_1$) and [X] is the concentration of free calcium in the dialysate. Model II allowed for heterogeneous and cooperative binding of calcium to the pair of sites in a domain.

$$\bar{Y}_{II} = \frac{K_1[X]^1 + 2K_2[X]^2}{2(1 + K_1[X]^1 + K_2[X]^2)} \quad (5)$$

The macroscopic equilibrium constant K_1 represents the sum of two intrinsic equilibrium constants (k_1 and k_2) that are not necessarily equal, and K_2 represents the equilibrium constant ($k_1k_2k_{12}$) for binding ligand to both sites; it accounts for any positive or negative cooperativity, regardless of its source or magnitude. It is not possible analytically to determine an estimate of the intradomain cooperativity, K_c, from these data alone; it may be estimated by assuming that the binding sites have equal intrinsic affinities ($K_1 = k_1 + k_2 = 2k$). This leads to a lower limit value of cooperativity, given by

$$K_c = 4K_2/(K_1)^2 \quad (6)$$

To accommodate the experimental data without prior normalization, the function used for fitting the data to each model was

$$F(X) = Y_{[X]_{low}} + \bar{Y}_j \cdot \text{span} \quad (7)$$

where $\bar{Y}_j$ refers to fractional saturation in model I or II as defined by eq 4 or 5 and was written in Fortran as a function of free energies rather than equilibrium constants. Note that the value of the parameter $Y_{[X]_{low}}$ corresponds to the value of the experimental signal (susceptibility or fluorescence) at the lowest calcium concentration in the range of abscissa values being fit, and the value of the parameter span is positive for a monotonically increasing signal. (At the limit of high ligand concentration, the experimental signal is equal to the sum of these two parameters.) This is equivalent to fitting for low and high end points.

Model-dependent analyses of the proteolytic susceptibility and fluorescence profiles of calcium titrations were conducted exhaustively over a wide range of starting guesses for the parameter values. In addition, multiple combinations of numerical constraints were applied to the free energies or normalization parameters (approximately 100 fits for each data set). In all of the analyses reported in Tables 1 and 2, association free energies were optimized parameters. Convergence was obtained for each combination of values using at least three sets of starting guesses that differed by 2 kcal/mol. Even when the midpoint is well-defined for a titration curve, slight variations in values of end points may dramatically affect the shape of the best-fit curve for any particular model (Johnson & Frasier, 1985). Thus, the parameters for end points were estimated simultaneously with those for free energies whenever possible.

In some cases, the limits of the titration curves were not sufficiently well-defined to solve simultaneously for both end point parameters ($Y_{[X]_{low}}$ and span) as well as the free energies or binding. To explore their effect on estimates of total free energy of binding and cooperativity, one or both of these parameters were set to a wide range of constant values ("fixing" them), while the remaining parameters were fit ("floated"). In all cases, fixing the end point parameters narrowed the confidence intervals resolved for the free energies (data not shown).

Multiple criteria were used for evaluating goodness-of-fit for the parameters that minimized the variance in each case. These error statistics as reported by *nonlin* included (a) the value of the square root of variance, (b) the values of asymmetric 65% confidence intervals, (c) the systematic trends in the distribution of residuals, (d) the magnitude of the span of residuals, and (e) the absolute value of elements of the correlation matrix.

RESULTS

The goal of these studies was to develop EndoGluC footprinting as a quantitative method to probe the calcium-dependent structural changes in calmodulin. The results presented here provide new insights into the ways that heterogeneous, cooperative calcium binding drives conformational switching of calmodulin, and they demonstrate the validity and limitations of this quantitative proteolytic footprinting approach.

Discontinuous Equilibrium Titrations. To resolve the energetics of calcium binding to calmodulin, it was essential to probe an equilibrium distribution of calmodulin species in a solution of known free calcium concentration. However, numerous technical difficulties in calculating free calcium levels have been recognized [e.g., Bers (1982)]. For the buffers used in this study, Figure 2b compares the experimentally determined pCa values and those calculated using published calcium and proton association constants for each component in the buffer (Fabiato & Fabiato, 1979; Sillen & Martell, 1971), their concentrations in the buffers (assuming purity based on information from manufacturer), and the total calcium concentration based on an experimental determination using atomic absorption spectroscopy. Although agreement was generally good, the greatest deviations between calculated and experimentally determined values occurred in a range where calmodulin binds calcium (~1 μM), as well as at the low calcium extreme. This was unacceptable; errors of this magnitude would affect both the position and shape of the resolved curve, changing estimates of total binding free energy and cooperativity. Thus, all of the pCa values reported for buffers used in this study were determined experimentally using BAPTA, difluoro-BAPTA, a calcium-selective electrode, or a combination of two methods as described in Experimental Procedures.

In order to reliably quantify the UV signal during HPLC analysis of peptide products, the calmodulin concentration had to be high (~15 μM). Because the dissociation constants for calcium binding are in the range of 1 μM, direct titration of a 15 μM calmodulin solution would have been in the regime of stoichiometric binding. Thus, it was impossible to perform an *equilibrium* titration of calmodulin by the addition of calcium to a single protein solution. Instead, by extensive dialysis of calmodulin against the individual pCa/pH buffers described earlier, we created a series of calmodulin solutions at equilibrium over a wide range of calcium concentrations. Thus, each datum in a footprinting or fluorescence titration represented the study of an individual dialysate and was independent of the data at other values of pCa.

Intrinsic Fluorescence of Equilibrium Titrations. The intrinsic tyrosine fluorescence of calmodulin dialysates at each of the 19 pCa levels was determined; normalized fluorescence values are shown in Figure 3. These values provide an independent indicator of the calcium-dependent structural changes of calmodulin and corroborate ordering of the buffers on the basis of experimental pCa determina-

Table 1: Model-Dependent Analyses of Calmodulin Titrations[a] Resolved from the Tyrosine Fluorescence and Susceptibility of E87-A88[b]

	model I	model II					
signal	ΔG_1[c]	ΔG_1[c]	ΔG_2	ΔG_c[d]	$Y_{[X]_{low}}$[e]	span[e]	$\sqrt{var}$[f]
Tyr fluor[g]	-8.15 ± 0.11				-0.08 ± 0.05	1.10 ± 0.05	0.065
		-7.50 ± 0.35	-16.41 ± 0.08	-2.2 ± 0.8	-0.01 ± 0.02	0.95 ± 0.03	0.023
E87 (1−87)	-8.47 ± 0.13				0.498 ± 0.033	-0.534 ± 0.029	0.051
		-8.00 ± 0.90	-16.96 ± 0.22	-1.8 -1.8, $+0.8$	0.486 ± 0.014	*(−0.500)*	0.040
E87 (88−148)	-8.55 ± 0.12				0.237 ± 0.015	-0.254 ± 0.013	0.022
		-8.31 ± 0.49	-17.09 ± 0.18	-1.3 -1, $+0.6$	0.233 ± 0.007	*(−0.244)*	0.018

[a] Model I assumed equal and independent binding; model II allowed heterogeneous and cooperative binding. [b] Data spanned the free calcium range from 7.3 nM to 0.34 mM (pCa 8.14−3.47). [c] All free energies are expressed on kilocalories/mole (1 kcal = 4.184 J). To overestimate the uncertainty in fitted values, the greater of the positive or negative limit of each asymmetric 65% confidence interval was tabulated. Unless reported individually, these differed by less than 2-fold. [d] Estimate of cooperative free energy was calculated as $\Delta G_c = \Delta G_2 - 2\Delta G_1 - RT \ln(4)$, and errors were propagated by *nonlin*; this formulation assumes that the intrinsic binding energies are equal (which was not assumed in the fits for ΔG_1 and ΔG_2) and gives a lower limit of the value of actual cooperativity. Asymmetric confidence intervals are shown if they differed by more than 2-fold. [e] Values in italics in parentheses were fixed during simultaneous fits for other parameter(s). [f] Values of the square root of the variance reflect differences in the span of the dependent variable in each data set because data were not normalized. Correlation coefficients, magnitude, and distribution of residuals were also evaluated but are not shown; for all data sets, fits to model I showed nonrandom residuals. [g] Tyrosine fluorescence.

Table 2: Model-Dependent Analyses of Calmodulin Titrations[a] Resolved from the Susceptibility of E31-L32[b]

	model I	model II					
range	ΔG_1[c]	ΔG_1	ΔG_2	ΔG_c[d]	$Y_{[X]_{low}}$[e]	span[e]	$\sqrt{var}$[f]
pCa 8.14−5.99[g]	-8.42 ± 0.16				0.037 ± 0.19	*(0.400)*	0.037
		-7.51 ± 0.75	-16.75 ± 0.14	-2.6 ± 1.4	0.059 ± 0.15	*(0.400)*	0.024
pCa 5.99−3.47[h]	-7.55 ± 0.20				0.406 ± 0.026	*(−0.400)*	0.047
		-6.51 ± 0.95	-15.05 ± 0.10	-2.85 ± 1.5	*(0.406)*	*(−0.400)*	0.034

[a] Model I assumed equal and independent binding; model II allowed heterogeneous and cooperative binding. [b] Data spanned the free calcium range from 7.3 nM to 1.02 μM (pCa 8.14−5.99) for the induced susceptibility portion of the E31 analysis; data spanned the free calcium range from 1.02 μM to 3.47 mM (pCa 5.99−3.47) for the induced protection portion of the E31 analysis. [c] All free energies are expressed in kilocalories/mole (1 kcal = 4.184 J). To overestimate the uncertainty in fitted values, the greater of the positive or negative limit of each asymmetric 65% confidence interval was tabulated. Unless reported individually, these differed by less than 2-fold. [d] Estimate of cooperative free energy was calculated as $\Delta G_c = \Delta G_2 - 2\Delta G_1 - RT \ln(4)$, and errors were propagated by *nonlin*; this formulation assumes that the intrinsic binding energies are equal (which was not assumed in the fits for ΔG_1 and ΔG_2) and gives a lower limit of the value of actual cooperativity. Asymmetric confidence intervals are shown if they differed by more than 2-fold. [e] Values in italics in parentheses were fixed during simultaneous fits for other parameter(s). [f] Values of the square root of the variance reflect differences in the span of the dependent variable in each data set because data were not normalized. Correlation coefficients, magnitude, and distribution of residuals were also evaluated but are not shown; for all data sets, fits to model I showed nonrandom residuals. [g] Induced susceptibility phase. [h] Induced protection phase.

tions. These data were analyzed according to both model I (eq 4), specifying equal, independent binding sites, and model II (eq 5), allowing heterogeneous, cooperative binding. Resolved parameters are listed in Table 1. The dialysates of calmodulin spanned a sufficiently wide range of free calcium such that, in fitting both models I and II, the parameters $Y_{[X]_{low}}$ and span (eq 6) could be floated simultaneously with the free energies (ΔG_1 and/or ΔG_2). Titration curves simulated using the best-fit values are shown in Figure 3a. Figure 3b shows the calculated values of the residuals for this fit to model I; by visual inspection, it is evident that they were systematic (nonrandom), indicating that the model itself was incorrect. As is characteristically seen in a fit of cooperative data to an independent binding site model, to fit the midpoint of the transition precisely, the fitted end points spanned a range beyond that defined by the experimental data.

As judged by criteria such as the square root of variance (a factor of 3 lower) and the smaller span and more random distribution of residuals (Figure 3b), these fluorescence data fit better to binding model II, which allowed heterogeneous and cooperative binding. The best-fit macroscopic free energies are given in Table 1. If one assumes that the binding sites have equivalent intrinsic calcium binding properties, then a lower limit on the actual cooperativity may be calculated by eq 6; as listed in Table 1, this corresponds to a factor of 43.

EndoGluC Activity and Exposure. For the proteolytic susceptibility profiles to merit consideration as equilibrium titration isotherms, many experimental variables such as exposure conditions and calcium-dependent effects on proteolytic catalysis were evaluated. A small chromogenic substrate for EndoGluC, Z-FLE-NA, was used to examine the dependence of protease activity on calcium concentration. As can be seen in Figure 2c, there is no systematic trend to the data. Thus, EndoGluC activity was independent of calcium concentration, and no corrections were applied.

The substrate Z-FLE-NA was added to each footpriting reaction as an internal standard to control for variations in the extent of exposure to protease. The average fraction of Z-FLE-NA cleaved was 12% ± 2% in the 45 separate footprinting reactions (Figure 2c). The value of fractional cleavage of Z-FLE-NA was determined for each footprinting reaction and used to normalize the fractional area of individual peptide peaks in that chromatogram, as described in eq 3 in Experimental Procedures.

Observed Cleavage Sites. Under these buffer conditions, EndoGluC specifically cleaves peptide bonds C-terminal to glutamate residues; no cleavage is expected between pairs of glutamate residues (Wilkinson, 1986; Beaudet *et al.*,

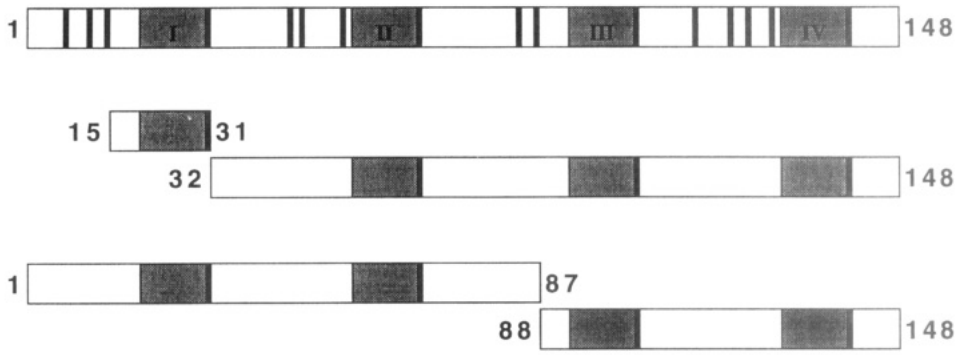

FIGURE 4: Cleavage products isolated after EndoGluC footprinting of calmodulin. The diagram indicates the four calcium binding sites. Major products were uncut calmodulin (1−148) with all possible cleavage sites marked. Products analyzed quantitatively are shown (15−31, 32−148, 1−87, 88−148); three of those were primary cleavage products.

1974). Of the 21 glutamate residues in calmodulin, only 16 are expected to be susceptible to EndoGluC because there are three occurrences of EE and one of EEE in the sequence (see Figure 1a). Under the conditions of limited proteolysis described earlier, cleavage was observed at a small subset of these 16 glutamate residues. At very low levels of proteolysis (less than 15%, leaving greater than 85% calmodulin whole), cleavage at only five of the possible sites was observed.

The observed fragments represented both primary and secondary cleavage products; they resulted from cuts at glutamate residues E14, E31 (site I), E87, E104 (site III), and E140 (site IV). Peptides 15−31 and 32−148 were formed due to cleavage between E31 and L32 in the N-terminal domain (Figure 4). Complementary peptides 1−87 and 88−148 were formed by cleavage between E87 and A88 in the helix preceding site III (Figure 4). Small quantities of peptides 88−140, 88−104, and 105−140 were formed from subfragmentation of the C-terminal domain (as judged by comparing the sum of relevant peak areas to that of peptide 1−87). In experiments in which the extent of proteolysis was increased above 15%, cleavage was observed at other sites in the C-terminal domain (E114, E123, and E127), as well as at E67, the terminal glutamate in site II. Significant subfragmentation of the N-terminal domain was not observed until the fraction of calmodulin cleaved increased above approximately 50%.

Chromatographic Separation and Quantitation of Peptides. The technique of HPLC reproducibly monitored the abundance of peptide products from proteolytic footprinting of calmodulin titrations and facilitated identification of the peptide products. Figure 5a shows a complete chromatogram of a single footprinting reaction of calmodulin at pCa 8.1. Consistent with conditions of limited proteolysis, calmodulin was the most abundant component in the chromatogram; the peptide products were low in abundance and primarily high in molecular weight (as shown by longer retention times on the HPLC column). Peaks labeled Z, Z′, and Z″ are derived from the internal standard, Z-FLE-NA, and used for normalization as described in Experimental Procedures.

Calcium-dependent changes in the susceptibility of cleavage sites were evident as the change in the relative abundance of the peptide products. Figure 5b shows a comparison of a region of the chromatogram for one of the footprinting reactions for four of the fifteen dialysates. Peptides labeled B (88−148) and C (1−87) decreased in abundance as the calcium concentration increased from nanomolar to micro-

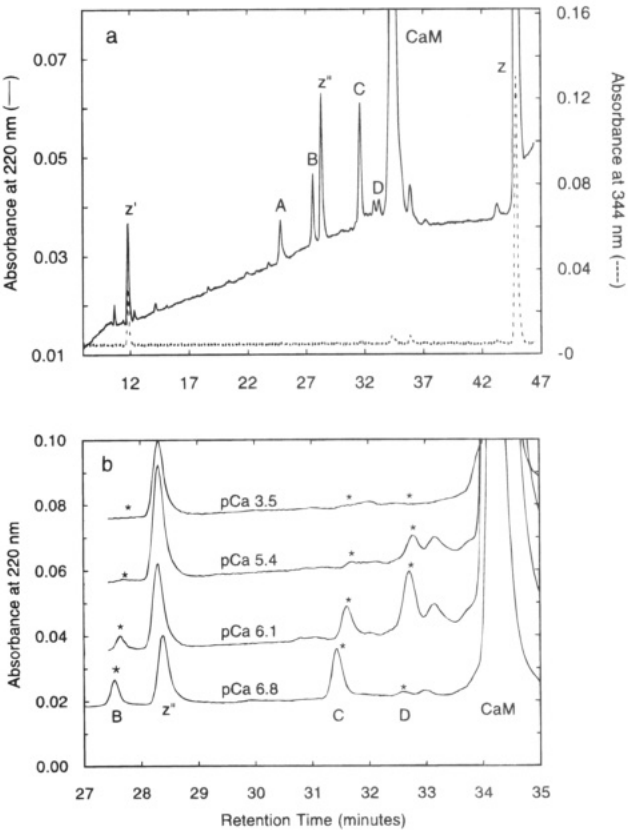

FIGURE 5: Separation by HPLC of fragments generated by EndoGluC footprinting of calmodulin. (a) Complete chromatogram from a single digest of dialysate pCa 8.1 monitored at 220 (solid line) and 344 nm (dashed line). Peak identities are as follows: Z′, Z-FLE-NA (cleaved: chromophore (NA) alone); A, peptide 88−140; B, peptide 88−148; Z″, Z-FLE-NA (cleaved: tripeptide (Z-FLE) alone); C, peptide 1−87; D, peptide 32−148; CaM, uncut calmodulin; Z, Z-FLE-NA (uncleaved). (b) Comparison of a region of the chromatogram from 27 to 35 min for footprinting reactions conducted at pCa 6.8, 6.2, 5.4, and 3.5 monitored at 220 nm; records are offset for clarity. Same peak labeling as that used in part a. Chromatographic conditions are described in the Experimental Procedures.

molar levels. This showed that the E87−A88 bond in the C-terminal domain was susceptible in apocalmodulin, but was protected from cleavage as calcium bound to calmodulin (Figure 6). (None of the fragments formed from subfragmentation of the C-terminal domain were detectable in footprinting reactions at calcium concentrations above 1 μM.)

The greatest surprise in these studies was that E31, the terminal glutamate in site I, showed biphasic susceptibility to EndoGluC proteolysis as calmodulin bound calcium, as

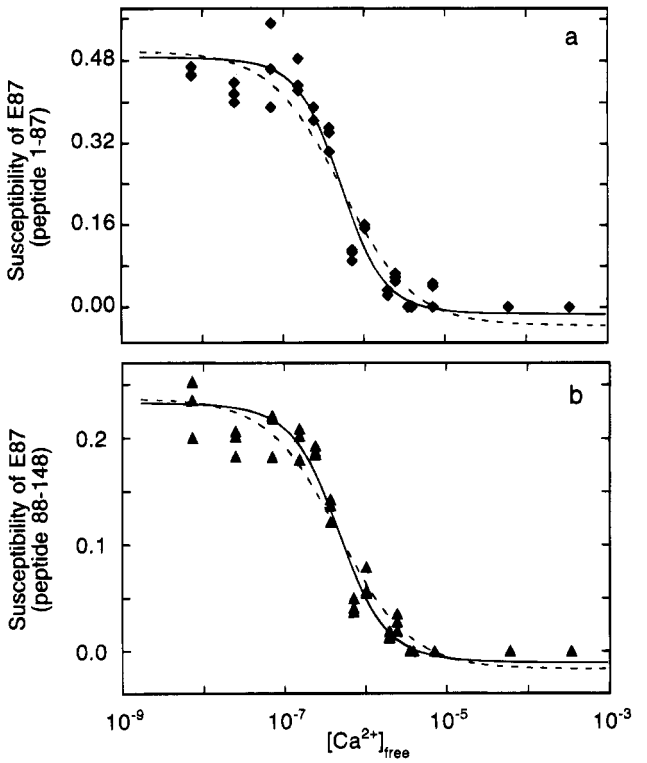

FIGURE 6: Susceptibility of the E87−A88 bond to cleavage by EndoGluC: comparison of the fractional abundance of complementary primary products, peptides 1−87 (a) and 88−148 (b), determined in triplicate footprinting reactions for each of 15 dialysates. (a) Fractional abundance of peptide 1−87 with curves corresponding to simulations using model I (eq 4, dashed line, ΔG_1 = −8.47 kcal/mol) or model II (eq 5, solid line, ΔG_1 = −8.00 kcal/mol, ΔG_2 = −16.96 kcal/mol). The Hill coefficient was 1.6. (b) Fractional abundance of peptide 88−148 with curves corresponding to simulations using model I (eq 4, dashed line, ΔG_1 = −8.55 kcal/mol) or model II (eq 5, solid line, ΔG_1 = −8.31 kcal/mol, ΔG_2 = −17.09 kcal/mol). The Hill coefficient was 1.5.

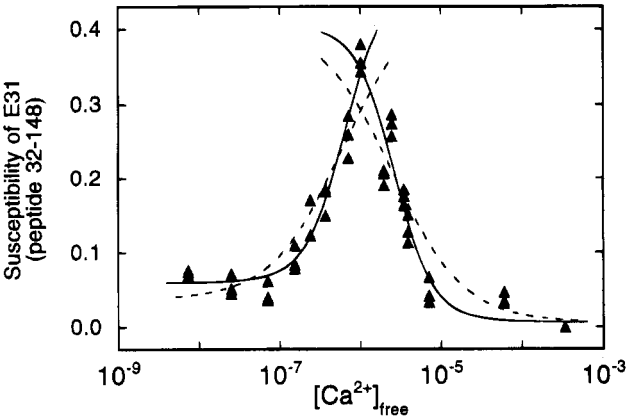

FIGURE 7: Susceptibility of the E31−L32 bond to cleavage by EndoGluC: comparison of the models for EndoGluC susceptibility at E31 (site I) fit piecewise to the biphasic abundance of peptide 32−148. In the range of pCa 8.14−6, curves correspond to simulations using model I (eq 4, dashed line, ΔG_1 = −8.42 kcal/mol) or model II (eq 5, solid line, ΔG_1 = −7.51 kcal/mol, ΔG_2 = −16.75 kcal/mol) according to fitted values in Table 2. In the range of pCa 6−3.47, curves correspond to simulations using model I (eq 4, dashed line, ΔG_1 = −7.55 kcal/mol) or model II (eq 5, solid line, ΔG_1 = −6.51 kcal/mol, ΔG_2 = −15.05 kcal/mol) according to fitted values in Table 2.

seen by the abundance of peptide D (32−148) in Figure 5b. It was not evident at low levels of free calcium, but increased in abundance in the range of nanomolar to micromolar free calcium; however, at higher calcium concentrations, the susceptibility of the E31−L32 bond was reduced and returned to being completely protected from cleavage in fully saturated calmodulin (Figure 7). As outlined in the following, these data were treated by piecewise analysis.

Nonlinear Least-Squares Analysis of Susceptibility Profiles. The fluorescent and footprinting titrations were analyzed according to the nature of the susceptibility profile (monotonic or biphasic). In all cases, the data were compared to two models of binding: one that forced equal and independent binding at two sites (model I) and the other that allowed heterogeneous and cooperative binding (model II). Note that the values of cooperative free energy, ΔG_c, that are reported in Tables 1 and 2 are not fit parameters. They were derived from the best-fit values of ΔG_1 and ΔG_2 in a fit to model II and then calculated by assuming that ΔG_1 representated two equal intrinsic free energies for calcium binding; errors in ΔG_1 and ΔG_2 were propagated.

Protection of E87-A88. Glutamate residue E87 is located in the C-terminal domain in the helix leading into site III. Over the course of the titration, the bond between E87 and A88 was protected monotonically from cleavage as calcium bound to calmodulin. In Figure 6, the fractional area of the peptide products 1−87 (Figure 6a) and 88−148 (Figure 6b) is shown as a function of the calcium concentration in each dialysate. It was possible to analyze the titration curves resolved from each peptide (1−87 and 88−148) individually. The scales for the corrected area, A_i', of each peptide differ because the absolute mass of peptide 88−148 was less than that of 1−87 due to its smaller molecular weight and slight subfragmentation. The mole fraction of peptide 88−148 and its subfragments (88−104, 105−140, 88−140) was equal to that of peptide 1−87.

Figure 6a shows data for peptide 1−87. These data were fit to models I and II, and comparisons were made with respect to simultaneously estimating (floating) or fixing the values of both $Y_{[X]_{low}}$ and span; best-fit values are reported in Table 1. The residuals of all fits to model I (equal and independent sites) showed sinusoidal variations characteristic of the mismatch between this model and a cooperative isotherm, as shown in Figure 3b for the fluorescence titration. This can be seen by visual inspection of the dashed curve in Figure 6a. Using model II, which allowed heterogeneous and cooperative binding, it was not possible to float the free energies and both $Y_{[X]_{low}}$ and span of these data; however, if one end point parameter was fixed, the other could be floated. The value estimated for the total free energy (ΔG_2) in the fits to model II did not change dramatically by fixing one or both end points, although the value of ΔG_1 was affected. The best-fit values are given in Table 2 and used to simulate the solid curve in Figure 6a. From inspection of the residuals and variance of the fits to models I and II (Table 1 and data not shown), it was apparent that the data were fit best by model II, which allowed for heterogeneous and cooperative binding.

Analysis of the calcium-dependent abundance of peptide 88−148 was performed in a fashion analogous to that described for peptide 1−87. There was a very slight difference between the model-dependent free energies resolved from the data for peptide 88−148 and those resolved from data for peptide 1−87. The value of ΔG_2 estimated for peptide 88−148 had a slightly lower value (more favorable binding affinity), but these differences were within

experimental error (0.1−0.2 kcal/mol). In all cases, the estimates for total free energy were lower (more favorable) than the best-fit values for tyrosine fluorescence (Table 1). However, the cooperative free energy was very similar. Thus, the susceptibility of the E87−A88 bond (Figure 6) reflected a cooperative binding event at a more favorable free energy than that resolved from tyrosine fluorescence data (Figure 3).

Induced Susceptibility of E31. Glutamate residue E31 is the bidentate chelator of calcium in site I. The susceptibility of the E31−L32 bond showed biphasic behavior (Figure 7); it was protected from cleavage at low and high calcium concentrations and showed the highest susceptibility to cleavage at intermediate calcium concentrations. The form of these data posed a significant challenge to nonlinear least-squares analysis; attempts to fit both phases simultaneously failed. Instead, the data were treated in a piecewise fashion. The dialysates between 7×10^{-9} and 1.02×10^{-6} M free calcium comprised the profile indicating increased susceptibility to proteolysis; those between 1.02×10^{-6} and 3.4×10^{-4} M free calcium were used to represent protection from proteolysis. The susceptibility values for the dialysate at 1.02×10^{-6} M calcium were included in both subsets of data to provide a constraint for continuity.

Each phase of the susceptibility data for E31 was fit to both models I and II (Table 2). When span and $Y_{[X]_{low}}$ were floated parameters, the resolved free energies were infinitely correlated. Thus, the value of either span or $Y_{[X]_{low}}$ was a fixed parameter in the fits; their values were chosen on the basis of the highest and lowest values of the independent variable. Because the data themselves did not permit an accurate estimate of the end point at maximal susceptibility, the effects of fixing $Y_{[X]_{low}}$ and span for these data at several different values were explored exhaustively (data not shown). A change in span from 0.4 to 0.5, for example, resulted in a change of only 0.5 kcal/mol in ΔG_2. (Note that the absolute values of susceptibility were not normalized for the length of the fragment; they were normalized only for the extent of proteolysis in that particular footprinting reaction.) Simulations using best-fit parameters (Table 2) are plotted in Figure 7. Given that both transitions are extremely steep, these data were expected and found to fit better to model II, which allowed heterogeneous and cooperative binding.

The most significant finding was the remarkable agreement between the values resolved for the induced susceptibility of E31 (Table 2) and the induced protection of E87 as monitored by peptides 1−87 and 88−148 (Table 1). This is evidence that susceptibility at E31 does not reflect the properties of binding at the nearest calcium binding site only.

Protection of E31. The susceptibility of E31 was maximal at approximately micromolar concentrations of free calcium. Subsequently the susceptibility was reduced, indicating protection of E31. This presumably arose because of calcium binding locally in the N-terminal domain, at site I or both sites I and II. From the piecewise analysis of the abundance of peptide 32−148, the total free energy (ΔG_2) was found to be ~2 kcal/mol less favorable than that observed for footprinting titrations corresponding to binding in the C-terminal domain. The calculated cooperativity was greater (ca. −3 kcal/mol); however, the error in that determination is large, reflecting the large uncertainty in ΔG_1. This is an extremely sharp, cooperative transition, making absolute values of ΔG_c imprecise.

Summary of Nonlinear Least-Squares Analysis. The model-dependent parameter estimates included in Tables 1 and 2 were drawn from a much larger set of analyses (>200). We used several criteria to judge these, including the dependence on starting guesses, the variance, the span and systematic nature of the residuals, the correlation of parameters, and the magnitude and symmetry of confidence intervals. In all cases, model II appeared to fit the data more closely and with fewer systematic (i.e., more random) residuals than did model I. In comparing the values of the square root of the variance, it is important to evaluate the trend for different fits to an individual set of data but not to compare values between data sets. This is because the susceptibility profiles were not normalized. Therefore, the value of the square root of the variance also indicates a difference in the numerical range of each data set. These values, expressed as a fraction of the span (e.g., 0.022/−0.254), are very similar (±5−10%) for all of the reported fits to EndoGluC footprinting reactions. All of the values for parameters reported in Tables 1 and 2 had correlation coefficients that were below 95%; in most cases, they were in the range of 40−70%.

DISCUSSION

Calmodulin is an essential, ubiquitous, and highly specific regulator of enzyme activity in most calcium-mediated pathways of signal transduction. Although calcium binding is understood to activate calmodulin for target recognition, many mysteries remain regarding its allosteric mechanism and the extent to which sites and domains interact [see Kilhoffer *et al.* (1992); Weinstein & Mehler, 1994; Cox, 1988; Wang, 1985]. A new appreciation for the division of labor between individual domains is emerging as calmodulin and its mutants are studied *in vivo* in organisms such as *Paramecium* (Kung *et al.*, 1992) and yeast (Davis, 1992; Ohya & Botstein, 1994) and as new structural studies of calmodulin complexes with target peptides are reported at a rapid pace [see Török and Whitaker (1994) for a review]. A complex interplay between site heterogeneity and cooperativity regulates four ligands binding to a protein of only 148 residues [see the Appendix of Haiech *et al.* (1981)].

To understand cooperative ligand binding fully, one must determine the number of populated intermediate (partially liganded) states and their energetic and structural relationship to the two end states, apocalmodulin and fully saturated calmodulin. One of the problems in understanding calmodulin is that there are no high-resolution studies of the structures adopted by apocalmodulin. Thus, it is not possible to postulate the mechanism of a cooperative binding process as the transition between known end states. Even if it were, it is instructive to review the case of hemoglobin, long a textbook paradigm for multisite cooperativity. Several critical elements of the molecular logic of this $\alpha-\beta-\alpha-\beta$ tetramer were overlooked in mechanisms based solely on detailed crystallographic structures of two end states. New experimental approaches that directly probed the intermediate states proved that the elegant and simple concerted (MWC) model for cooperativity was inadequate to explain the detailed logic of ligand-induced quaternary switching [see Ackers and Hazzard (1993)]. However, very few techniques have been developed that successfully quantitate the populations of intermediate states under equilibrium conditions, and

enormous effort is required to test the experimental validity of such methods [e.g., Brenowitz *et al.* (1986); Senear *et al.*, 1993].

One of the approaches to studying conformational switching in cooperative systems is to probe ligand-induced macromolecular susceptibility to limited cleavage or modification. These approaches have been used successfully to obtain two classes of information: mapping of susceptible positions and quantitative determinations of changes in the extent of susceptibility coupled to ligand binding. For example, proteolytic probe studies of cAMP binding to CRP (Heyduk & Lee, 1989) showed that three conformations were adopted, thus disproving an "all-or-none" (2-state) model of switching. Quantitative DNase footprint titrations (Brenowitz *et al.*, 1986) have been used to determine microscopic free energies of protein−DNA interactions; hydrogen exchange methods have been used to correlate local change with allosteric mechanisms [e.g., Englander *et al.* (1992)]. Such approaches have given estimates of the number of molecular conformations populated during cooperative ligand binding and the energetic costs of transitions between them.

In calmodulin, the susceptibility of lysine residues to proteolytic cleavage and chemical derivatization has been studied in this way. Partial proteolysis of calmodulin using trypsin indicated that cleavage occurred in a calcium-dependent fashion (Kawasaki *et al.*, 1986; Walsh *et al.*, 1977). Mackall and Klee (1991) interpreted their finding of the biphasic susceptibility of the central helix as indicating that apocalmodulin and fully saturated calmodulin adopted similar conformations, but that an intermediate of different structure was formed. Giedroc *et al.*, (1985, 1987) showed that the calcium-dependent reactivities of the two lysines in the central helix (K75 and K77) differed dramatically, in spite of their close proximity. To exploit these calcium-dependent differences in the environments of individual residues in calmodulin, we have developed the novel quantitative proteolytic footprinting method reported here.

In this study, EndoGluC has been used to monitor site occupancy and conformational change induced by cooperative calcium binding to calmodulin under equilibrium conditions. The ultimate goal of these studies was to determine which partially liganded species were populated and the rules for transition between them (i.e., the molecular partition function for calcium binding). The EndoGluC footprinting method has given insight into residue-specific differences between the intermediate states and into the microscopic equilibrium constants for intrinsic affinity and cooperative interactions of calcium binding.

This has allowed us to develop a model for conformational switching in which calmodulin ($\alpha-\beta-\alpha'-\beta'$) progresses through at least three distinct states in solution, corresponding to three levels of ligand binding. In this model, the ensemble of configurations adopted by apocalmodulin is characterized by intramolecular interactions; the N-terminal domain ($\alpha-\beta$) is relatively rigid, and the C-terminal segment (α') that comprises much of the central helix and contains site III is the most flexible. We postulate that the plasticity that characterizes the interactions of calmodulin with its cellular targets [see Meador *et al.* (1993)] may play a role in allowing many energetically equivalent forms of the apo state to coexist. At an intermediate state of saturation, with approximately two calcium ions bound, the interdomain interactions of the apo state(s) are modified. The C-terminal domain is more constrained by favorable intradomain interactions between sites III and IV, and the N-terminal domain becomes more flexible and accessible. In the third state, both calcium-saturated domains of calmodulin have less conformational flexibility, and interdomain interactions are altered and diminished. This structural interpretation of calcium-induced conformational change relies heavily on the quantitative EndoGluC footprinting and fluorescence studies presented here, as well as other proteolytic footprinting studies of calmodulin titrations. The following discussion addresses the related issues of (a) experimental validation of the EndoGluC footprinting method and (b) new information it has provided regarding the allosteric mechanism of calmodulin.

EndoGluC Footprinting Method. This technique was designed to take advantage of the properties of native calmodulin that change in response to calcium binding. Acidic residues play a key role in determining the calcium binding affinities of EF-hand sites [see Procyshyn and Reid (1994); Renner *et al.*, 1993; Marsden *et al.*, 1990]. In each site, the invariant terminal glutamate residue (E31, E67, E104, and E140, see Figure 1a) offers both of its side chain oxygens for bidentate chelation of the calcium ion; binding of calcium necessarily causes a significant reorientation of this residue. In addition to these four glutamate residues, seventeen others are distributed throughout the calmodulin sequence. Thus, EndoGluC was chosen as a suitable enzymatic probe of conformational change because it specifically cleaves peptide bonds that are C-terminal to glutamate residues. The terminal glutamate of each EF-hand site was expected to serve as a direct probe of site occupancy; the other glutamate residues are distributed globally (see Figure 1a), but were expected to be locally sensitive reporters of the structural transitions that occur upon calcium binding.

Quantitative susceptibility profiles were resolved for the cleavage at E87 and at E31. For model-dependent analysis of susceptibility profiles to be thermodynamically meaningful, the independent variable (i.e., free ligand) must be known accurately, and the dependent variable (i.e., susceptibility) must be related to calcium binding to calmodulin in a measurable way. Approaches developed for controlling the independent and dependent variables and other issues related to the validation of this footprinting method are discussed in the following.

To obtain a signal-to-noise ratio suitable for the accurate spectrophotometric quantitation of peptides, it was necessary to work with samples of calmodulin in the range of 15 μM (0.25 mg/mL). However, the dissociation constants for calcium binding to calmodulin are in the micromolar range. This ruled out the possibility of conducting a direct equilibrium titration by the simple addition of ligand. Instead, it was essential to equilibrate individual samples in individual pH/pCa buffers at high concentrations of calmodulin and to determine experimentally the concentration of free calcium in each one as described in the Experimental Procedures.

The buffer conditions were 50 mM HEPES and 94 mM KCl with 0.5 mM EGTA and 0.5 mM NTA. The concentrations of the chelators EGTA and NTA were adequate but not ideal for buffering calcium over the entire range (nanomolar to micromolar) required for these studies. As can be seen in Figure 2b, there were points of significant deviation between the calculated and experimentally determined free calcium concentrations of the buffers. Thus,

experimental determination of the free calcium concentration was required.

Several experimental factors were addressed directly in order to ensure that the footprinting titrations reflected the properties of calmodulin, rather than those of EndoGluC. These included determining whether the activity of EndoGluC was calcium-sensitive and controlling for experimental variations in extent and quenching of proteolysis. Digestion of Z-FLE-NA by EndoGluC was shown to be calcium-independent (Figure 2c); thus, the patterns of calcium-dependent susceptibility of calmodulin may be interpreted to indicate calcium-induced conformational changes, rather than altered proteolytic activity.

For the fractional susceptibility of a single bond to indicate a property of native calmodulin, the fragments formed must be primary cleavage products. The extent of cleavage never exceeded 15% for any footprinting reaction. To control for small variations in protease exposure in the individual footprinting reactions, the extent of proteolysis in each was determined by the addition of Z-FLE-NA.

Molecular Origins of Changes in Susceptibility—Conformational Change vs Binding. The experimental signal monitored by proteolytic footprinting is the change in backbone susceptibility of calmodulin as a function of calcium binding. The pure interpretation of that signal is that a conformational change in the side chain and/or backbone has occurred in response to binding. However, the signal may result from changes in the conformational entropy of the surrounding segment, the accessibility of the side chain, or in the peptide bond itself. If this conformational change or difference in accessibility is linearly related to the extent of binding, then the resulting profile represents an individual site isotherm. In a multisite protein, the median ligand concentration of such an isotherm represents the chemical work of saturation at that site, concurrent with binding at other sites, regardless of the degree of cooperativity and the heterogeneous nature of the sites (Wyman, 1964). It is clear, however, that changes in susceptibility do not arise solely from the changes in occupancy of the closest binding site(s).

It is important to recognize that this dilemma (a) is shared by many spectroscopic and chemical methods (e.g., hydrogen exchange) and (b) may be tractable, given sufficient independent determinations that each carry different systematic deviations. Techniques such as circular dichroism, fluorescence, and NMR have been productively applied to the study of calcium binding to calmodulin; they each have yielded insight into the average properties of the protein backbone or the nature of conformational changes in the vicinity of a few residues that provide unambiguous signals. Although there are few naturally occurring reporter groups in calmodulin, mutagenesis and chemical modification procedures have been applied to introduce them. Studies of such mutants have elucidated an ordered binding mechanism.

Kilhoffer and co-workers (1992) demonstrated that site heterogeneity and intradomain cooperativity in calmodulin were required for a consistent description of the fluorescent properties of calcium binding to five mutants of synthetic calmodulin (SYNCAM) engineered to have tryptophan at position 7 in one of the four calcium binding sites (T26W, T62W, Y99W, Q135W) or the central helix (S81W). This required that they assume that the mutations did not alter the binding properties. However, they pointed out that even when a unique, benign reporter group at a known location is monitored, site occupancy and associated conformational changes are not readily deconvolved. This difficulty in the interpretation of structural transitions that result from calcium binding is common to all chemical and spectroscopic probes of microscopic binding processes.

On the basis of these EndoGluC footprinting studies alone, it is not possible to determine independently the coefficients that relate binding to proteolytic susceptibility. For example, it could be that species with a particular number of ligands bound (zero, one, two, three, or four) each have a characteristic susceptibility; this would require the determination of at least five susceptibility coefficients. Alternatively, each of the 16 species that differ with respect to the position of ligand(s) might have a unique susceptibility coefficient. The nonlinear least-squares analysis has been conducted using the simple interpretation that susceptibility is linearly related to the extent of binding and has been designated as model-dependent for that reason. This interpretation may be tested by comparing these results with those obtained using residue-specific probes such as other proteolytic footprinting and spectroscopic techniques, as well as the macroscopic properties determined from equilibrium titrations monitored by flow dialysis (Crouch & Klee, 1980), or by using calcium chelators to monitor ligand dissociation rather than properties of calmodulin *per se* [e.g., Linse *et al.* (1991)]. In the discussion that follows, we comment on insights that have been gained regarding calcium binding and intra- and interdomain interactions using this method, the self-consistency of EndoGluC footprinting studies, and the degree to which these results supplement and extend previous understanding of the mechanism of cooperative calcium binding to calmodulin.

Cooperative Calcium Binding to Sites III and IV. The intrinsic tyrosine fluorescence of calmodulin primarily reflects a change in the environment of Y138 (in site IV), which has been shown to be relatively insensitive to calcium binding at the N-terminal sites I and II (Drabikowski *et al.*, 1977; Drabikowski & Brzeska, 1982; Wang *et al.*, 1982, 1984). Reported free energies resolved from titrations monitored by fluorescence vary from −15 (Drabikowski & Brzeska, 1982) to −18 kcal/mol (Wang *et al.*, 1982) under conditions similar, but not identical, to those used in this study. The median of the isotherm derived from changes in intrinsic tyrosine fluorescence (Figure 3) indicated a slightly lower affinity binding event (higher free energy) than that determined for the susceptibility of E87; the difference corresponded to 0.6 kcal/mol. Studies using NMR and proteases such as thrombin and bromelain (data not shown) to probe the dialysates comprising these equilibrium titrations of calmodulin suggest that this deviation of 0.6 kcal/mol represents a real difference in the calcium-linked conformational response of residues E87 and Y138 in the C-terminal domain.

The signals from E87 and Y138 may differ if they respond unequally to the same binding processes. It is not known to what degree the calcium-dependent change in intrinsic tyrosine fluorescence of Y138 reports on the individual occupancy of site IV or the average occupancy of both sites III and IV in the C-terminal domain. If it were more sensitive to the average properties of the domain (or the properties of site IV alone), and the susceptibility of E87 were more sensitive to the occupancy of site III, then the

simple conclusion would be that site III has a higher affinity for calcium than does site IV. A similar conclusion was reached by Kilhoffer *et al.* (1992). This hypothesis could be tested directly with wild-type calmodulin if it were possible to determine independently the contribution of each binding event to the total change in intrinsic tyrosine fluorescence. Studies are underway using the approach of Lohman and Bujalowski (1991) to determine the values for native calmodulin under these conditions. The most plausible explanation for differences seen between signals from E87 and Y138 is that sites III and IV do not have the same intrinsic affinity for calcium, and this is reflected in the extent and coupling of conformational change to binding.

The conclusion that two binding sites in the same domain may differ with respect to their intrinsic affinities for calcium (i.e., site III is not equivalent to site IV) is supported by equilibrium and kinetic studies of mutants of *Drosophila melanogaster* calmodulin in which the terminal glutamate of each binding site was replaced by lysine or glutamine. As expected, binding was reduced or eliminated in the mutant site (Maune *et al.*, 1992; Martin *et al.*, 1992). However, stoichiometric titrations of these mutants monitored by NMR indicated that while mutation of site III caused the affinity of site IV to drop and *vice versa*, mutation of site III did not have the same effect on site IV as mutation of site IV had on site III (Starovasnik *et al.*, 1992). Although the reduction in affinity could be explained solely by the loss of cooperative interactions between sites III and IV, the effect of a single mutation should have been equivalent (regardless of site) if the intrinsic affinities were equal and no other pairwise interactions were affected. Those nonreciprocal effects suggested that the intrinsic affinities of sites III and IV differed as also implied by the difference in signals from E87 to Y138.

There is remarkable agreement between the free energies resolved from the induced susceptibility of E31 (Table 2) and those from the protection of E87 (Table 1) in these EndoGluC footprinting reactions. This is a strong indication that the phase of the isotherm indicating induced susceptibility of E31 (Figure 7) is due to calcium binding in the C-terminal domain rather than to a nonspecific effect of calcium on the N-terminal domain. The free energy resolved from this phase of the data for E31 (see Table 2) may most accurately represent the total free energy for two calcium ions binding to the C-terminal domain. The resolved value of ΔG_2 falls between the free energies resolved from EndoGluC footprinting at E87 and from tyrosine fluorescence of Y138 (Table 1), as would be expected if they represented the occupancy of sites III and IV, respectively.

The isotherms that resulted from calcium binding in the C-terminal domain indicated intradomain cooperativity, as well as heterogeneity of calcium binding affinities. This conclusion is based on several factors, including the span and systematic nature of the residuals from fits to model I, which indicated that an independent binding model was insufficient to describe the process. The values of cooperative free energy, ΔG_c, calculated from the susceptibility data at E87 and the tyrosine fluorescence of Y138 are very similar, as are the Hill coefficients (noted in the legends to Figures 3 and 6). The exact shapes of the transitions and, therefore, the extent of resolved cooperativity are highly dependent on an accurate estimate of the concentration of free ligand. Given that the footprinting and fluorescence measurements were made on the same equilibrated dialysates of calmodulin, the free calcium concentration is assured of being identical in the two titrations. With confidence in the absolute values of those determinations, the agreement between methods and the values of cooperative free energy resolved may be taken as significant.

It is not possible to determine whether the susceptibility of the E87−A88 bond is influenced by calcium binding to N-terminal sites, which might confer the additional protection of that bond. Note that there is incomplete separation of the signals pertaining to each domain; the inflection point in the susceptibility profile for E31-L32 occurs at a concentration of free calcium lower than that required for complete protection of E87. The extended dumbbell structure (see Figure 1b) resolved from crystallographic studies of calcium-saturated calmodulin would suggest that there is no significant physical interaction between domains, and thus, this overlap in titration curves arises solely from the degree of separation in values of free energies of intrinsic binding and intradomain cooperativity. However, molecular models such as CAM10 (Pascual-Ahuir *et al.*, 1991) and experimental studies of calmodulin (Persechini & Kretsinger, 1988; Small & Anderson, 1988; Török *et al.*, 1992; Heidorn & Trewhella, 1988) suggest that a more compact structure for calcium-saturated calmodulin is energetically favorable and would allow for interdomain interactions to contribute to a change in chemical or spectroscopic signal. The degree to which calcium binding to the N-terminal domain contributes to the susceptibility at E87 cannot be assessed from these data alone.

Interdomain Interactions. The most striking feature of the EndoGluC footprinting reactions of calmodulin titrations was the biphasic nature of the susceptibility of the peptide bond C-terminal to glutamate 31 (E31−L32). This was an entirely unexpected result. Given that E31 is the bidentate chelator of calcium in site I, it should be an exquisitely sensitive indicator of binding in that site. However, most bonds in calmodulin are protected from proteolysis upon binding of calcium, and the sites in the N-terminal domain were recognized as having a lower affinity for calcium than those in the C-terminal domain; therefore, we expected a monotonic response having a higher median ligand concentration, indicating a lower affinity for calcium.

Instead, the susceptibility of the bond between E31 and L32 changed in two phases. It was (a) protected from proteolysis in apocalmodulin, (b) became susceptible coincident with the protection of E87, and (c) became protected at higher calcium levels, presumably as calcium bound to site I and was chelated by the oxygen atoms OE1 and OE2 of E31. Although opposite in sign, these two phases of increasing and decreasing susceptibility were equal in magnitude. There was no plateau between the transitions representing induced susceptibility and protection. Given that the sites in the C-terminal domain are those with higher affinity, propagated conformational change is the most plausible explanation for the induced susceptibility of the E31−L32 bond in the N-terminal domain. The incontrovertible evidence of a biphasic response provides compelling support for the existence of at least one intermediate form of calmodulin, whose properties are significantly different from those of both the apo and fully saturated forms and is not an average of the two end states. Although E31−L32 was protected in both the apo and fully saturated states, the

structural origins for this protection must differ given the change in occupancy of site I and the side chain interactions of E31. Furthermore, because E31 is not in the central helix, it suggests that calcium binding to sites III and IV affects the conformation of the entire N-terminal domain, not just the portion that comprises the interface between the domains.

Most studies have concluded that there is little or no interaction between the N-terminal and C-terminal domains of calmodulin in the absence of target peptides or drugs. This conclusion is based largely on comparisons of titration curves for whole calmodulin to additive reconstruction of those of the isolated domains (Dalgarno *et al.*, 1984; Aulabaugh *et al.*, 1984; Ikura *et al.*, 1984). However, Maune *et al.* (1992) and Beckingham (1991) noted that mutations in one domain increased the affinity of sites in the other, suggesting anti-cooperativity in the native protein. Biphasic tryptic susceptibility of the central helix near K75 (Mackall & Klee, 1991) agrees with our findings, if interpreted as indicating that the interface between domains changes in an ordered, calcium-dependent way. Early NMR studies by Seamon (1980) conclusively showed that the greatest change in chemical shifts of Y99 and Y138 occurred in response to the first two calcium ions binding, but additional change occurred upon binding the second pair of calcium ions. Fluorescence studies showed that terbium binding to N-terminal sites changed calcium binding to C-terminal sites (Wang *et al.*, 1984). The UV absorbance of calmodulin changes most upon binding two calcium ions to calmodulin, but continues to change in the range of 2−4 calcium ions binding (Klee, 1977; Yazawa *et al.*, 1990). It is not known whether this is because of direct interactions between the domains or because binding to the C-terminal sites is not complete before N-terminal sites begin to saturate.

In these EndoGluC footprinting studies, the only direct indicator of calcium binding in the N-terminal domain was the phase of decreasing susceptibility of E31-L32 (in the range between 1.02 μM and 0.34 mM free calcium). The total free energy, ΔG_2, resolved from this transition was estimated to be approximately 1.5−2 kcal/mol less favorable than those of C-terminal sites (−15.05 *vs* −16.95 for E87 or −16.41 kcal/mol for Y138). Model-dependent analysis of each phase of the E31 susceptibility profile required that at least one of the end points be fixed; the estimate of the total free energy varied only slightly, but the calculated value of cooperativity (ΔG_c) was very sensitive to changes in end points. Although the absolute value of ΔG_c was not well-determined, the transitions clearly are positively cooperative.

If we assume that binding of calcium at site I protects the E31−L32 bond from cleavage, this transition may represent an individual site isotherm (Ackers *et al.*, 1983) of site I with fractional protection proportional to fractional occupancy. It is possible that a fraction of the protection of E31-L32 results from conformational changes induced by binding at site II in the absence of binding at I. In addition, we cannot eliminate the possibility that binding at sites III and IV in the C-terminal domain plays a role in the protection at E31.

The simplest explanation, however, is that the biphasic behavior reflects transitions between a series of distinct structures, in which (a) the F helix of site I is stabilized by intramolecular interactions in the absence of calcium, (b) some of these constraints are released upon calcium binding to sites III and IV, and (c) different constraints are assumed upon calcium binding to the N-terminal sites I and II. Proteolytic footprinting studies of isolated domains of calmodulin are being used to address this hypothesis directly (data not shown).

The EndoGluC footprinting titrations corroborate other studies of calmodulin that have shown that calcium binding induces at least one intermediate conformation [e.g., Crouch and Klee (1980); Seamon, 1980]. The distinction is that the results presented here strongly suggest that, in the absence of bound calcium, the domains of calmodulin interact with each other despite their flexibility. Such interactions between domains would provide a conformational explanation for the anti-cooperativity, or energetic barrier, to calcium binding inferred from the studies of mutants of *D. melanogaster* calmodulin containing only three functional sites (Maune *et al.*, 1992; Martin *et al.*, 1992). Evidence for interactions provides constraints on the nature of the populated intermediate states and energetic rules for transitions between them.

The detailed structural nature of residue-specific interactions has yet to be elucidated. Heteronuclear NMR methods (Ikura *et al.*, 1991) applied to $(Ca^{2+})_4$-CaM showed that a segment (residues 78−81) of the central helix defined by the crystallographic structure was disordered (see Figure 1a). Although NMR studies have not reported specific residue interactions (e.g., NOEs) between the two domains in the absence of target peptides, biphasic behavior (one domain responding to a binding event in the other domain) has been observed for several resonances, including H107 (Evans *et al.*, 1988) and T26 (Starovasnik *et al.*, 1992), under stoichiometric binding conditions. These results indicated that the domains do not function completely independently of one another, even though they retain very similar fundamental structures and macroscopic calcium binding properties as isolated half-molecules (Klee, 1988).

Consistency of Resolved Free Energies. Confidence in the quantitative EndoGluC footprinting of calmodulin titrations requires that self-consistency be evaluated by comparing the abundance of complementary cleavage products. If the susceptibility of an individual peptide bond reflects a property of whole calmodulin, then the molar abundance of complementary primary fragments should be equivalent and analysis of their profiles should yield equal free energies. This was true for the peptides representing cleavage at E87-A88 (comprising residues 1−87 and 88−148), as shown in Figure 6 and Table 1; the best-fit values of ΔG_1 were within 0.1 kcal/mol. Similarly, self-consistency was found for products of cleavage at E31: residues 15−31 (data not shown) and 32−148 (Figure 7). These agreed with each other; both products displayed biphasic behavior with similar medians for each of the transitions. Thus, it appears that the susceptibility profiles of E31 and E87 reflect calcium-dependent properties of whole calmodulin, as was the aim.

We have used several proteases other than EndoGluC (a serine protease) to probe calcium binding to calmodulin; abstracts of early stages in the development of these footprinting studies have appeared previously (Pedigo *et al.*, 1991; Schaller & Shea, 1992; Verhoeven & Shea, 1993). The susceptibility profiles resulting from footprinting with bromelain (a cysteine protease) and thrombin (a serine protease) have been analyzed quantitatively in the same manner as reported here (data not shown), corroborating the results obtained using EndoGluC. The susceptibility of E87 to bromelain decreased monotonically in response to calcium

binding; the resolved free energy, ΔG_2, from that study (-17.1 ± 0.2 kcal/mol) is identical to that derived from susceptibility to EndoGluC (see Table 1). The susceptibilities of R37 to thrombin and of S38 to bromelain were biphasic, as observed for E31. Resolved free energies from piecewise analysis of the R37 and S38 isotherms corroborate the interpretation of the data reported here. The excellent agreement between residue-specific responses of calmodulin, as monitored by very different proteases, confirms the assertion that the behavior of calmodulin, and not the protease, is reflected in the calcium-dependent properties of these footprinting titrations.

The free energies for calcium binding resolved from EndoGluC footprinting titrations are consistent with other studies showing differences between the domains (Klee, 1988; Drabikowski & Brzeska, 1982; Starovasnik *et al.*, 1992; Wang *et al.*, 1984). Although the EndoGluC footprinting studies here resolved domain free energies, their sums agree well with macroscopic free energies determined in other studies (Crouch & Klee, 1980; Maune *et al.*, 1992; Martin *et al.*, 1992; Linse *et al.*, 1991).

Calmodulin as a Substrate of EndoGluC. The conformational heterogeneity of calmodulin is reflected in the subset of bonds susceptible to EndoGluC, as well as their calcium-dependent responses as described earlier. EndoGluC has been used previously to digest calmodulin fully for chemical analysis (Schaefer *et al.*, 1987a,b). To our knowledge, this study is the first report of its relative preference for bonds of calmodulin and its use to detect calcium-linked conformational changes of calmodulin. The susceptibility of a peptide bond to proteolytic cleavage depends on both its accessibility (i.e., position relative to the surface) and its intrinsic suitability as a substrate for the protease. This may depend on the conformational flexibility of the local region of the protein and specific chemical contacts with side chains of several nearby residues. EndoGluC is not highly selective (Wilkinson, 1986; Beaudet *et al.*, 1974), although it does not cleave between neighboring glutamate residues. Of the 21 glutamate residues in the calmodulin sequence (see Figure 1a), 16 precede bonds that are expected to be targets of EndoGluC. The subset of susceptible bonds suggests that conformations adopted over the course of calcium binding differ significantly from the one seen in the crystal structure resolved for fully saturated calmodulin.

Under the conditions of limited proteolysis used in these footprinting reactions (<15% calmodulin cleaved), only five of the sixteen bonds were observed to be susceptible. There was no apparent sequence preference for the two neighboring residues; bonds C-terminal to E14 (KEA), E31 (KEL), E87 (REA), E104 (AEL), and E140 (EEF) were cleaved. Neither the reported sequence specificity of EndoGluC nor the high-resolution structures of calcium-saturated calmodulin (Babu *et al.*, 1988; Ikura *et al.*, 1991) provide an obvious explanation for the relative preference for these positions. Conservation of mass, as measured by the sum of peak areas in the chromatogram (values not shown), argued that no highly abundant, large peptides were overlooked in our analysis. The most straightforward interpretation of preferential cleavage is that the five susceptible bonds conformationally differed from the eleven others that were not cleaved over the course of the titration.

On the basis of the structures (see Figure 1b) determined by crystallographic and NMR methods, all five bonds are located in regions expected to be helical in the calcium-saturated state of calmodulin. In that state, all of these were protected from proteolysis by EndoGluC. Protection at a high degree of calcium saturation is probably due to a calcium-induced decrease in conformational flexibility as well as changes in secondary structure *per se*, as has been seen using NMR to study ion binding to the two EF-hand sites of calbindin (Akke *et al.*, 1993). Susceptibility at lower calcium levels argues that the conformation of the scissile bond is not rigidly helical over the course of a titration.

As an indicator of residue flexibility, the temperature factors of the calcium-saturated structure (Babu *et al.*, 1988) were compared. Most residues in the N-terminal domain have lower *B*-factors than those in the C-terminal domain, as expected on the basis of its greater rigidity. However, there was no simple correlation between the *B*-factors for glutamate residues (main chain or side chain values) and susceptibility to EndoGluC. Although several factors such as multiple conformers [e.g., Borgstahl *et al.* (1994)] may contribute to the value of a temperature factor, this lack of correspondence implies that relative properties of the glutamate residues in apocalmodulin or partially saturated calmodulin are not fully represented by the structure of $(Ca^{2+})_4$-CaM shown in Figure 1b.

It would be preferable to compare apo and saturated sites. The only crystallographic study of a pair of apo EF-hand sites is of sites I and II in half-saturated (two Ca^{2+}) troponin C (5tnc.pdb; Herzberg & James, 1988). As expected, the *B*-factors of residues in the apo EF-hand sites are higher (by approximately 2-fold) than those of the saturated sites. But within each site, there is a clear hierarchy such that the first six residues have higher *B*-factors than the last six, regardless of the presence of calcium. This may reflect the dominant helix-forming propensity of SXXE and TXXE capping boxes (Harper & Rose, 1993) that stabilize helical secondary structure and may contribute to the protection of E31 (in a TTKE sequence) in the absence of a calcium ligand.

The preference of EndoGluC for five of the sixteen expected sites in calmodulin may be interpreted in terms of the relative calcium-dependent flexibility of the surrounding regions of calmodulin and the calcium affinities of nearby sites. It appears that the primary sequence of 12 residues in an EF-hand site is a critical, but not exclusive, determinant of calcium affinity (Marsden *et al.*, 1990; McPhalen *et al.*, 1991). The structures adopted by the chelating residues of calcium-saturated sites are nearly identical, as judged by the superposition of domains from related proteins such as calmodulin and troponin C. Thus, the differences in free energies of binding may indicate that major differences lie in the apo states. Although it is possible to rationalize the relative calcium affinities of some EF-hand sites on the basis of the small differences in the coordinates of the chelating residues (Nayal & di Cera, 1994), the exact positions of the those residues depend on interactions outside the site, as well as within it (Waltersson *et al.*, 1993). These comparisons suggest that the flexibility and interactions of connecting loops and helices of the protein must contribute to optimal coordination geometry. EndoGluC appears to probe these differences.

In the EndoGluC footprinting studies, the relative flexibility of the apo C-terminal domain ($\alpha'-\beta'$) was reflected by cleavage at E87 *vs* complete protection of E31 in the N-terminal domain ($\alpha-\beta$). Other studies of apocalmodulin

have noted the proteolytic lability of the C-terminal domain (Mackall & Klee, 1991; Walsh *et al.*, 1977; Kawasaki *et al.*, 1986) and its lower melting temperature, as determined by differential scanning calorimetry (Tsalkova & Privalov, 1985). Spectroscopic studies indicate that calcium loading of the C-terminal domain causes the largest structural change in calmodulin [see Klevit (1983) for a review], suggesting that it is less constrained in the absence of calcium. As an isolated domain, it also has a higher affinity for calcium than does the N-terminal domain. It appears that the flexibility of the apo form of the C-terminal domain is a determinant of its higher calcium affinity relative to the N-terminal domain.

The observed preference for a subset of five out of the sixteen possible positions of cleavage by EndoGluC suggests unanticipated differences in the local structure of glutamate residues in corresponding locations in each of the four helix−loop−helix segments of calmodulin. For example, E123 is in a position relative to site IV that is equivalent to E87 relative to site III. However, it is not a primary cleavage product. When the extent of proteolysis was increased above approximately 15% (data not shown), subsequent subfragmentation occurred at E104, E140, and additional positions (E114, E123, E127).

These results suggest that, despite the similarities among the primary sequences of the four covalently connected helix−loop−helix segments ($\alpha-\beta-\alpha'-\beta'$) of calmodulin, the segment containing site III (α') seems to be the most flexible. This interpretation is supported by studies (Ota & Clarke, 1989, 1994; Potter *et al.*, 1993) showing that calcium binding affects the spontaneous degradation of Asp and Asn residues in the EF-hand sites of calmodulin. Site III was the most susceptible to degradation, followed by sites IV and II, and calcium binding protected the sites from degradation. This suggested that site III is the most disordered apo site and that it is measurably different from site IV in the same domain, consistent with the pattern of cleavage by EndoGluC.

In combination with the footprinting studies reported here on apocalmodulin, these results suggest that the lower susceptibility of regions outside of α' indicates rigidity, either intrinsic to the sequence or caused by stabilizing interactions within calmodulin. It is possible that, in the apo form, the third segment is not stably folded and that calcium binding causes folding and therefore protection. This interpretation is also consistent with chemical denaturation studies of calmodulin under these conditions (data not shown). Proteolytic susceptibility studies used to monitor local regions undergoing helix−coil transitions (Ueno & Harrington, 1984) or to determine flexible regions or autonomous subdomains in protein folding [e.g., Wu *et al.* (1994)] have emphasized the linkage between folding and ligand binding in other systems. They support the view that a functional (native) form may be partially unfolded or highly disordered in an internal region, as may be true for apocalmodulin.

In contrast to the C-terminal domain, the average structure of the N-terminal domain changes little in response to calcium binding (Klevit, 1983; Klevit *et al.*, 1984; Dalgarno *et al.*, 1984; Drabikowski & Brzeska, 1982; Klee, 1977). The protection or lack of susceptibility of E31 in the apo state corroborates the relative rigidity of the N-terminal domain. The susceptibility of E31−L32 at intermediate calcium levels indicates a reversible change in the local conformation or accessibility of this bond to EndoGluC. Either or both of these require the formation of an intermediate species different from both the apo and calcium-saturated forms.

Much as the understanding of cooperativity in the hemoglobin tetramer has focused on understanding rearrangements of the dimer−dimer ($\alpha^1-\beta^2$) interface, so does our interest in calmodulin naturally focus on understanding the forces that drive secondary and tertiary changes in the interface between the two domains, as well as within domains. Although it is possible to frame questions about the structures of calmodulin and its allosteric mechanism in terms of the structure of the central helix *per se*, its conformation is a consequence of the calcium-induced changes in the structural disposition of the β and α' segments (see Figure 1). Rather than treating the central helix as an independent structural unit that serves to connect two globular domains, we view it as primarily comprising elements intrinsic to those globular domains (the F helix of site II in segment β and the E helix of site III in segment α') connected by a flexible loop that may adopt a nearly helical structure. A model for transitions is given in the following.

Model of Calmodulin Switching. The quantitative EndoGluC footprinting method described here has been developed to probe calcium-induced conformational changes at a residue-specific level and to dissect the roles of individual structural elements and the energies of intrinsic and cooperative interactions. The most astonishing finding was that the E31−L32 bond responded to calcium binding to sites III and IV in the absence of local (N-terminal) calcium binding.

On the basis of the susceptibility of E31-L32 and E87-L88 to EndoGluC, we conclude that, in the absence of calcium, the α' segment is relatively disordered and the domains interact interact in ways that protect segments α, β, and β' from cleavage. These constraints evidently are disrupted by calcium binding to sites III and IV, while new interactions may occur between the two domains. Although it is possible that a conformational change in the C-terminal domain could be propagated through a stiff central helix, it is difficult to rationalize this on the basis of the structure of $(Ca^{2+})_4$-CaM, as shown in Figure 1b. The distances between the Cα atom of E31 and the calcium ions in the C-terminal domain are approximately 43.5 Å (site III) and 42 Å (site IV), which are not plausible distances for specific, long-range interactions. This suggests that some conformations adopted by calmodulin must differ from the one shown in Figure 1b and may be more similar to those proposed by Kretsinger (1992a). Although the molar basis for the interdomain interactions cannot be deduced from this study alone, a changing pattern of electrostatic and hydrophobic interactions is expected to play a prominent role.

Studies of calcium-dependent changes in the conformations of E31-L32 and E87-A88 reported here may be summarized by using the truth table below (eq 8) correlating the susceptibility (1) or protection (0) of a bond to EndoGluC cleavage with the number of calcium ions bound. This chart includes the response of R37, as probed by thrombin, and I125, as probed by bromelain (data not shown), to draw attention to the consistency of residue-specific responses within a single helix in the first segment, α, and comparison between those in different segments (i.e., α *vs* β' and α' *vs* β').

	α E31	α R37	α′ E87	β′ I125
apo (0)	0	0	1	0
partial (~2)	1	1	0	1
saturated (4)	0	0	0	0

Note that an identical response does not necessarily arise for identical reasons (i.e., protection (0) afforded by calcium binding cannot be responsible for the protection of an apo segment).

This pattern of susceptibility leads to a proposal that (a) calmodulin adopts at least three states that are conformationally distinct, (b) the conformation of apo-α′ (containing site III) is measurably more flexible and susceptible than that of the other three, and (c) the segments α, β, and β′ (containing sites I, II, and IV, respectively) interact with each other. Each of these proposed states is expected to represent an ensemble of energetically accessible microstates that meet the boundary conditions of susceptibility defined by these proteolytic footprinting studies.

If all apo segments were similarly flexible and calcium binding had equivalent structural consequences on their proteolytic susceptibility, the transition of the α−β−α′−β′ sequence might have been represented as being (a) most susceptible in the apo state (1-1-1-1), (b) partially protected once the C-terminal domain was saturated (1-1-0-0), and (c) fully protected (0-0-0-0) upon complete saturation. This expectation would provide for three states of the interface between N- and C-terminal domains, as required by previously published studies of stoichiometric and equilibrium titrations. However, it would provide for only two states of each domain proper, (0-0) or (1-1). This pattern was not observed. Instead, each domain makes two transitions coupled to changes in the other domain.

SUMMARY

The allosteric mechanism of calcium binding to calmodulin has been the subject of intense study for almost 2 decades. The small size of this protein belies the difficulty of discerning the molecular logic of its cooperative calcium binding transitions. Despite elegant structural studies of the calcium-saturated form of calmodulin and very precise thermodynamic and kinetic characterizations of the macroscopic calcium binding properties, the number of intermediate states and the roles of individual structural elements in defining them are not fully understood.

The EndoGluC footprinting studies, while probing only a few positions in calmodulin, have given unique insights into the molecular logic of this very efficient and complex protein. It has allowed the study of the allosteric mechanism of calcium binding without introducing mutations or covalent reporter groups. A favorable comparison with the extensive literature on calcium binding to calmodulin supports the assertion that the EndoGluC footprinting method is valid for monitoring microscopic binding properties quantitatively as well as qualitatively. The chemical basis for all of the observed changes in susceptibility has yet to be determined. The model presented here for calcium-induced conformational switching proposes three conformations that are distinguishable in their patterns of intra- and interdomain interactions. This raises additional questions that may be tested further by many methods.

ACKNOWLEDGMENT

The authors thank Gilson Medical Electronics for the donation of the autosampler unit for the HPLC used in this study; R. Mauer and P. Howard (University of Oregon) for the overexpression vector used for calmodulin; A. Bergold and K. Wright (University of Iowa College of Medicine Protein Structure Facility) for amino acid analysis and N-terminal sequencing; D. Moser (University of Iowa DNA Core) for DNA sequencing; R. Rogers and S. Riahi (University of Iowa College of Medicine, Department of Pediatrics) for the use of an atomic absorption spectrometer; and the reviewers for helpful suggestions.

REFERENCES

Abola, E., Bernstein, F. C., Bryant, S. H., Koetzle, T. F., & Weng, J. (1987) in *Crystallographic Databases—Information Content, Software Systems, Scientific Applications* (Allen, F. H., Bergerhoff, G., & Sievers, R., Eds.) pp 107−132, Data Commission of International Union of Crystallography, Bonn.

Ackers, G. K., & Hazzard, J. H. (1993) *Trends Biochem. Sci. 18*, 385−390.

Ackers, G. K., Shea, M. A., & Smith, F. R. (1983) *J. Mol. Biol. 170*, 223−242.

Akke, M., Skelton, N. J., Kördel, J., Palmer, A. G., III, & Chazin, W. J. (1993) *Biochemistry 32*, 9832−9844.

Aulabaugh, A., Niemczura, W. P., & Gibbons, W. A. (1984) *Biochem. Biophys. Res. Commun. 118*, 225−232.

Babu, Y. S., Bugg, C. E., & Cook, W. J. (1988) *J. Mol. Biol. 204*, 191−204.

Barbato, G., Ikura, M., Kay, L. E., Pastor, R. W., & Bax, A. (1992) *Biochemistry 31*, 5269−5278.

Beaudet, R., Saheb, S. A., & Drapeau, G. R. (1974) *J. Biol. Chem. 249*, 6468−6471.

Bernstein, F. C., Koetzle, T. F., Williams, G. J. B., Meyer, E. F., Jr., Brice, M. D., Rodgers, J. R., Kennard, O., Shimanouchi, T., & Tasumi, M. (1977) *J. Mol. Biol. 112*, 535−542.

Bers, D. M. (1982) *Am. J. Physiol. 242*, C404−C408.

Borgstahl, G. E. O., Rogers, P. H., & Arnone, A. (1994) *J. Mol. Biol. 236*, 817−830.

Brenowitz, M., Senear, D. F., Shea, M. A., & Ackers, G. K. (1986) *Methods Enzymol. 130*, 132−181.

Cohen, P., & Klee, C. B. (Eds.) (1988) *Calmodulin*, Elsevier, New York.

Cox, J. A. (1988) *Biochem. J. 249*, 621−629.

Crouch, T. H., & Klee, C. B. (1980) *Biochemistry 19*, 3692−3698.

Dalgarno, D. C., Klevit, R. E., Levine, B. A., Williams, R. J. P., Dobrowolski, Z., & Drabikowski, W. (1984) *Eur. J. Biochem. 138*, 281−289.

Davis, T. N. (1992) *Cell Calcium 13*, 434−444.

Drabikowski, W., & Brzeska, H. (1982) *J. Biol. Chem. 257*, 11584−15590.

Drabikowski, W., Kuznicki, J., & Grabarek, Z. (1977) *Biochim. Biophys. Acta 485*, 124−133.

Englander, S. W., Englander, J. J., McKinnie, R. E., Ackers, G. K., Turner, G. J., Westrick, J. A., & Gill, S. J. (1992) *Science 256*, 1684−1687.

Evans, J. S., Levine, B. A., Williams, R. J. P., & Wormald, M. R. (1988) in *Calmodulin* (Cohen, P., & Klee, C. B., Eds.) pp 57−82, Elsevier, New York.

Fabiato, A., & Fabiato, F. (1979) *J. Physiol. 75*, 463−505.

Finn, B. E., Drakenberg, T., & Forsén, S. (1993) *FEBS Lett. 336*, 368−374.

Giedroc, D. P., Sinhas, S. K., Brew, K., & Puett, D. (1985) *J. Biol. Chem. 260*, 13406−13413.

Giedroc, D. P., Puett, D., Sinha, S. K., & Brew, K. (1987) *Arch. Biochem. Biophys. 252*, 136−144.

Haiech, J., Klee, C. B., & Demaille, J. G. (1981) *Biochemistry 20*, 3890−3897.

Harper, E. T., & Rose, G. D. (1993) *Biochemistry 32*, 7605−7609.

Heidorn, D. B., & Trewhella, J. (1988) *Biochemistry 27*, 909−915.

Herzberg, O., & James, M. N. G. (1988) *J. Mol. Biol. 203*, 761−779.
Heyduk, T., & Lee, J. C. (1989) *Biochemistry 28*, 6914−6924.
Hoffman, R. C., & Klevit, R. E. (1991) *Tech. Protein Chem. II* 383−391.
Ikura, M., Hiraoki, T., Hikichi, K., Minowa, O., Yamaguchi, H., Yazawa, M., & Yagi, K. (1984) *Biochemistry 23*, 3124−3128.
Ikura, M., Spera, S., Barbato, G., Kay, L. E., Krinks, M., & Bax, A. (1991) *Biochemistry 30*, 9216−9228.
Johnson, M. L., & Frasier, S. G. (1985) *Methods Enzymol. 117*, 301−342.
Kawasaki, H., Kurosu, Y., Kasai, H., Isobe, T., & Okuyama, T. (1986) *J. Biochem. (Tokyo) 99*, 1409−1416.
Kilhoffer, M.-C., Kubina, M., Travers, F., & Haiech, J. (1992) *Biochemistry 31*, 8098−8106.
Klee, C. B. (1977) *Biochemistry 16*, 1017−1024.
Klee, C. B. (1988) in *Calmodulin* (Cohen, P., & Klee, C. B., Eds.) pp 35−56, Elsevier, New York.
Klevit, R. E. (1983) *Methods Enzymol. 102*, 82−104.
Klevit, R. E., Dalgarno, D. C., Levine, B. A., & Williams, R. J. P. (1984) *Eur. J. Biochem. 139*, 109−114.
Kraulis, P. J. (1991) *J. Appl. Crystallogr. 24*, 946−950.
Kretsinger, R. H. (1976) *Annu. Rev. Biochem. 45*, 239−265.
Kretsinger, R. H. (1992a) *Science 258*, 50−51.
Kretsinger, R. H. (1992b) *Cell Calcium 13*, 363−376.
Kung, C., Preston, R. R., Maley, M. E., Ling, K.-Y., Kanabrocki, J. A., Seavey, B. R., & Saimi, Y. (1992) *Cell Calcium 13*, 413−425.
LaPorte, D. C., Weirman, B. M., & Storm, D. R. (1980) *Biochemistry 19*, 3814−3819.
Linse, S., Helmersson, A., & Forsen, S. (1991) *J. Biol. Chem. 266*, 8050−8054.
Lohman, T. M., & Bujalowski, W. (1991) *Methods Enzymol. 208*, 258−290.
Mackall, J., & Klee, C. B. (1991) *Biochemistry 30*, 7242−7247.
Marsden, B. J., Shaw, G. S., & Sykes, B. D. (1990) *Biochem. Cell Biol. 68*, 587−601.
Martin, S. R., Andersson-Teleman, A., Bayley, P. M., Drakenberg, T., & Forsén, S. (1985) *Eur. J. Biochem. 151*, 543−550.
Martin, S. R., Maune, J. F., Beckingham, K., & Bayley, P. M. (1992) *Eur. J. Biochem. 205*, 1107−1114.
Maune, J. F., Klee, C. B., & Beckingham, K. (1992) *J. Biol. Chem. 267*, 5286−5295.
McPhalen, C. A., Strynadka, N. C. J., & James, M. N. G. (1991) *Adv. Protein Chem. 42*, 77−144.
Meador, W. E., Means, A. R., & Quiocho, F. A. (1993) *Science 262*, 1718−1721.
Moncrief, N. D., Kretsinger, R. H., & Goodman, M. (1990) *J. Mol. Evol. 30*, 522−562.
Nayal, M., & di Cera, E. (1994) *Proc. Natl. Acad. Sci. U.S.A. 91*, 817−821.
Ohya, Y., & Botstein, D. (1994) *Science 263*, 963−966.
Ota, I. M., & Clarke, S. (1989) *Biochemistry 28*, 4020−4027.
Ota, I. M., & Clarke, S. (1994) *J. Biol. Chem. 264*, 54−60.
Pascual-Ahuir, J.-L., Mehler, E. L., & Weinstein, H. (1991) *Mol. Eng. 1*, 231−247.
Pedigo, S., Verhoeven, A. S., Schaller, W. A., & Shea, M. A. (1991) *Biophys. J. 59*, 23a.
Persechini, A., & Kretsinger, R. H. (1988) *J. Biol. Chem. 263*, 12175−12178.
Potter, S. M., Henzel, W. J., & Aswad, D. W. (1993) *Protein Sci. 2*, 1648−1663.
Procyshyn, R. M., & Reid, R. E. (1994) *J. Biol. Chem. 269*, 1641−1647.
Putkey, J. A., Slaughter, G. R., & Means, A. R. (1985) *J. Biol. Chem. 260* (8), 4704−4712.
Renner, M., Danielson, M. A., & Falke, J. J. (1993) *Proc. Natl. Acad. Sci. U.S.A. 90*, 6493−6497.
Schaefer, W. H., Hinrichsen, R. D., Burgess-Cassler, A., Kung, C., Blair, I. A., & Watterson, D. M. (1987a) *Proc. Natl. Acad. Sci. U.S.A. 84*, 3931−3935.
Schaefer, W. H., Lukas, T. J., Blair, I. A., Schultz, J. E., & Watterson, D. M. (1987b) *J. Biol. Chem. 262*, 1025−1029.
Schaller, W. A., & Shea, M. A. (1992) *Biophys. J. 61*, A211.
Seamon, K. B. (1980) *Biochemistry 19*, 207−215.
Senear, D. F., Dalma-Weiszhausz, D. D., & Brenowitz, M. (1993) *Electrophoresis 14*, 704−712.
Sillen, L. G., & Martell, A. E. (1971) *Stability Constants of Metal-Ion Complexes: Special Publication No. 25 of The Chemical Society*, Alden & Mowbray, Ltd., Oxford, UK.
Small, E. W., & Anderson, S. R. (1988) *Biochemistry 27*, 419−428.
Starovasnik, M. A., Su, D.-A., Beckingham, K., & Klevit, R. E. (1992) *Protein Sci. 1*, 245−253.
Swenson, C. A., & Fredricksen, R. S. (1992) *Biochemistry 31*, 3420−3429.
Tabor, S., & Richardson, C. C. (1985) *Proc. Natl. Acad. Sci. U.S.A. 262*, 1074−1078.
Török, K., Lane, A. N., Martin, S. R., Janot, J.-M., & Bayley, P. M. (1992) *Biochemistry 31*, 3452−3462.
Török, K., & Whitaker, M. (1994) *BioEssays 16* (4), 221−224.
Tsalkova, T. N., & Privalov, P. L. (1985) *J. Mol. Biol. 181*, 533−544.
Ueno, H., & Harrington, W. F. (1984) *J. Mol. Biol. 173*, 35−61.
Verhoeven, A. S., & Shea, M. A. (1993) *Biophys. J. 64*, A169.
Walsh, M., Stevens, F. C., Kuznicki, J., & Drabikowski, W. (1977) *J. Biol. Chem. 252*, 7440−7443.
Waltersson, Y., Linse, S., Brodin, P., & Grundström, T. (1993) *Biochemistry 32*, 7866−7871.
Wang, C.-L. A. (1985) *Biochem. Biophys. Res. Commun. 130* (1), 426−430.
Wang, C.-L. A., Aquaron, R. R., Leavis, P. C., & Gergely, J. (1982) *Eur. J. Biochem. 124*, 7−12.
Wang, C.-L. A., Leavis, P. C., & Gergely, J. (1984) *Biochemistry 23*, 6410−6415.
Weinstein, H., & Mehler, E. L. (1994) *Annu. Rev. Physiol. 56*, 213−236.
Wilkinson, J. M. (1986) in *Practical Protein Chemistry—A Handbook* (Darbre, A., Ed.) pp 121−148, John Wiley and Sons Ltd., New York.
Wu, L. C., Gradori, R., & Carey, J. (1994) *Protein Sci. 3*, 369−371.
Wyman, J., Jr. (1964) *Adv. Protein Chem. 19*, 223−286.
Yazawa, M., Matsuzawa, F., & Yagi, K. (1990) *J. Biochem. (Tokyo) 107*, 287−291.

BI941624I